

Active-fire landscapes demonstrate structural resistance to subsequent fire and drought

Caden P. Chamberlain ^{a,b,*}, Liz van Wagtendonk ^a, Bryce N. Bartl-Geller ^a,
Malcolm P. North ^c, C. Alina Cansler ^d, Marc D. Meyer ^e, Chad T. Anderson ^f, Van R. Kane ^a

^a School of Environmental and Forest Sciences, University of Washington, Seattle, WA 98195, USA

^b Colorado Forest Restoration Institute, Colorado State University, Fort Collins, CO 80524, USA

^c USDA Forest Service, Pacific Southwest Research Station, Davis, CA 95618, USA

^d W.A. Franke College of Forestry & Conservation, University of Montana, Missoula, MT 59812, USA

^e USDA Forest Service, Region 5 Ecology Program, Southern Sierra Province, Mammoth Lakes, CA 93546, USA

^f National Park Service, Yosemite National Park, El Portal, CA 95318, USA

ARTICLE INFO

Keywords:

Drought
Dry forests
Fire
Forest structure
Lidar
Resilience
Resistance

ABSTRACT

A key tenet of contemporary management in dry, fire-adapted forests of western North America is the reintroduction of a frequent and low- to moderate-severity fire regime. Where this fire regime has been fully or partially restored, it is critical to evaluate the degree to which these landscapes demonstrate forest structural resistance (i.e., the capacity to retain intrinsic structures through time) under novel climates and disturbances. In this study, we used overlapping airborne lidar datasets spanning active-fire landscapes in the Sierra Nevada, California, to evaluate how tree densities, clumping patterns, and height distributions changed during a decade of moderate-intensity wildfires and extreme drought. We evaluated structural resistance in landscapes affected by drought alone (drought-only) and by the combination of drought and wildfire (drought-fire) and examined how patterns of change varied across pre-disturbance conditions. We observed moderately high landscape-scale resistance of structural patterns during the extreme 2012–2016 drought, with only 5 % loss of trees > 32 m. Structural changes in the drought-fire context were more pronounced (25 % total tree loss); however, medium-sized (16–32 m) and tall (>32 m) trees as well as 1–4 and 5–9 tree clumps, demonstrated relatively high resistance at the landscape scale. Structural changes in the drought-only context were primarily associated with cooler and wetter microclimates. In the drought-fire context, structural changes occurred primarily in sites with higher pre-disturbance canopy cover (>40 %), in more exposed topographic positions, and where time since past fire was longer (16 + years). Overall, results from our study suggest that management practices that restore active-fire conditions in dry forest landscapes are likely to increase the resilience and adaptive capacity of these ecosystems.

1. Introduction

Fires were excluded from most forest ecosystems of western North America for at least a century following Euro-American colonization (Marlon et al., 2012; Hagmann et al., 2021). However, recognizing the critical role of fire in fire-adapted forests (Falk et al., 2011; McLaughlin et al., 2020), national-level policies now promote prescribed burning and resource objective wildfires (i.e., fires managed under a non-full suppression strategy) across many federally managed landscapes (Stephens et al., 2016a; Huffman et al., 2020; North et al., 2024). Historically, through a negative feedback with fuels, frequent and low- to

moderate-severity fires promoted dry forest resistance (Hessburg et al., 2019); that is, the capacity of forest ecosystems to retain their intrinsic structures and compositions through subsequent disturbances and climatic variations (Walker et al., 2004; Falk et al., 2022). Yet as fires return to dry forest landscapes, uncertainties remain regarding the structural resistance of *contemporary* active-fire landscapes under shifting climatic conditions and novel disturbance regimes (Larson et al., 2013; Pawlikowski et al., 2019).

Wildfire, drought, and bark beetles are primary disturbance agents in dry forests, each having unique impacts on structures and compositions, and together defining complex and interacting disturbance regimes

* Corresponding author.

E-mail address: caden.chamberlain@colostate.edu (C.P. Chamberlain).

(Larson and Churchill, 2012; Hessburg et al., 2019). Individual disturbances can mediate or amplify the likelihood, magnitude, and effects of subsequent disturbances, and multiple short-interval disturbances can have compounding effects on vegetation, sometimes exceeding the impacts of single disturbance events (Johnstone et al., 2016; Kane et al., 2017; Steel et al., 2023). With climate change likely to increase the interaction and compounding effects of disturbances in dry forests ecosystems (Buma, 2015; Westerling, 2016; Schoennagel et al., 2017), it is critical to evaluate the resistance of active-fire landscapes under these changing conditions.

Historically, fire-intact ecosystems contained a mix of structural features that were either resistant (i.e., persisted through disturbances) or temporally dynamic (i.e., were more likely to experience change from disturbance) (Larson and Churchill, 2012; Lloret et al., 2012). At fine spatial scales, large- and medium-sized fire-resistant pines, arranged primarily as single trees and small clumps of trees, were capable of persisting through multiple low-intensity disturbances (Keey, 2012; Falk et al., 2022). Intermixed within these resistant structural features were more dynamic structures including cohorts of small- and medium-sized trees, sometimes forming large contiguous tree clumps, that were more readily consumed by fires (Mast and Veblen, 1999; Abella and Denton, 2009; Larson and Churchill, 2012). Droughts and associated bark beetle outbreaks could be widespread but typically had isolated effects on structures, occasionally killing mature trees within large clumps (Churchill et al., 2013; Das et al., 2016). Across broader spatial extents, vegetation dynamics varied by past disturbance intensity and underlying biophysical conditions creating heterogenous structural patterns across forest landscapes (e.g., higher tree densities in wetter microclimates and lower densities in drier sites) (Collins et al., 2007, 2015; Hessburg et al., 2015; Safford and Stevens, 2017).

Dry forest ecosystems within California's Sierra Nevada have been impacted extensively by wildfires in recent decades (Cova et al., 2023; Williams et al., 2023). In some landscapes, where recent fires have had mostly low- and moderate-severity effects, active-fire conditions similar to the historical fire regime of these forests have begun to reestablish (Collins et al., 2016; Jeronimo et al., 2019; Hankin et al., 2022; Chamberlain et al., 2023b). Recent work indicates that structural patterns in these partially-restored active-fire landscapes resemble aspects of the resistant structures that historically characterized these forests, with relatively low tree densities, low and variable surface fuel loading (Collins et al., 2011a, 2016; Lydersen et al., 2014), and heterogenous vegetation patch arrangements at multiple spatial scales (Kane et al., 2013; 2014; Jeronimo et al., 2019; Ng et al., 2020; Chamberlain et al., 2023a). However, while structural patterns in partially-restored active-fire landscapes generally align with historical conditions, these sites may still exhibit the residual effects of fire suppression, with higher tree densities and fuel loading, and misaligned species distributions (Lydersen et al., 2014; May et al., 2023). As such, it remains particularly valuable to evaluate the resistance and structural dynamics of these partially-restored, active-fire landscapes as they face novel conditions under climate change.

Numerous recent studies quantified patterns and mechanisms of tree-level mortality in active-fire landscapes during the 2012–2016 drought in the Sierra Nevada. Across the region, drought severity aligned with elevational and latitudinal gradients, with generally higher mortality rates observed in the lower montane zone in the southern Sierra Nevada (Young et al., 2017; Fettig et al., 2019). Mediating these broad climatic drivers of mortality were more site-specific influences of past management, fire history, and forest structural patterns (Young et al., 2017; Restaino et al., 2019; Furniss et al., 2022). For example, several studies found that past restoration thinning and prescribed burning treatments, which reduce tree densities and competition, tended to mitigate mortality during the 2012–2016 drought (Restaino et al., 2019; Knapp et al., 2021), though primarily in less climatically stressed sites (Steel et al., 2021b). Boisramé et al. (2017) and Furniss et al. (2022) also reported reduced mortality rates in the mid- and upper-montane forests in

Yosemite National Park with recent histories of frequent low- and moderate-severity fire (i.e., resembling the historical fire regime). Fewer studies have assessed how tree-level mortality rates from the 2012–2016 drought scaled up to influence stand- to landscape-scale structural patterns and resistance (though see Young et al. 2020 and Furniss et al. 2022).

Forests impacted from California's 2012–2016 drought were, or soon will likely be, impacted by wildfire, resulting in instances of interacting disturbances and potential for compounding effects. Kane et al. (2015a) and Lydersen et al. (2014) used satellite-derived burn severity indices to evaluate structural resistance following drought and fire in active-fire landscapes in the Sierra Nevada. Their results generally showed that active-fire landscapes burned at low- and moderate-severity in subsequent fires (at least under non-extreme fire weather conditions), indicating moderate resistance of upper canopy cover (during the early years of the 2012–2016 drought). Hankin and Anderson (2022) used airborne lidar data to evaluate how vegetation height distributions varied by fire history characteristics in Yosemite National Park, finding that both upper and lower strata canopy structures tended to stabilize (i.e., demonstrate resistance) after two low-intensity fires (Hankin et al., 2022; 2024). Furthermore, in the Ishi Wilderness in northern California, Pawlikowski et al. (2019) showed that large individual trees and small tree clumps demonstrated the greatest resistance during subsequent fires in a partially fire-restored landscape, though their analyses did not evaluate resistance under interacting drought and fire disturbances.

In this study, we leveraged two overlapping airborne lidar datasets from 2010 and 2019 to track changes in fine-scale tree spatial patterns and height distributions through contemporary disturbance regimes in an active-fire landscape in Yosemite National Park. We then assessed how structural changes varied across gradients of fire history and biophysical conditions. Our study focused on the historically fire-adapted yellow pine and mixed-conifer (YPMC) forests within the study area. We use the term “resistance” to refer to the stability of structural patterns across the landscape. We addressed two primary research questions:

1. How did total tree density, tree clumping patterns, and tree height distributions change in a single disturbance (drought-only) and dual disturbance (drought and wildfire) context?
2. How did pre-disturbance fire history, biophysical setting, and forest structural patterns influence structural changes in each disturbance context?

2. Methods

We mapped drought-only and drought-fire settings across all YPMC forests in our study area. We used 2010 and 2019 airborne lidar acquisitions to quantify key fine-scale forest structure metrics including total tree density and the proportion of total density by tree clump size and height class. Linear models and generalized linear models (GLMs) were used to evaluate changes in forest structural conditions in each disturbance context, while holding key climatic and topographic factors constant (Objective 1). We then produced structural change metrics by differencing 2019 and 2010 conditions and used generalized additive models (GAMs) to identify relationships between these change metrics and key environmental variables including fire history, climate, topography, and pre-disturbance forest structure (Objective 2). We performed all primary analyses in R (R Core Team 2024).

2.1. Study area

We defined our study area based on the overlapping footprints of the 2010 and 2019 airborne lidar acquisitions, representing a 10,631-ha region within Yosemite National Park in the central Sierra Nevada, California, USA (Fig. 1a-d). The study area is characterized by a Mediterranean climate. Mean annual precipitation ranges from 971 to

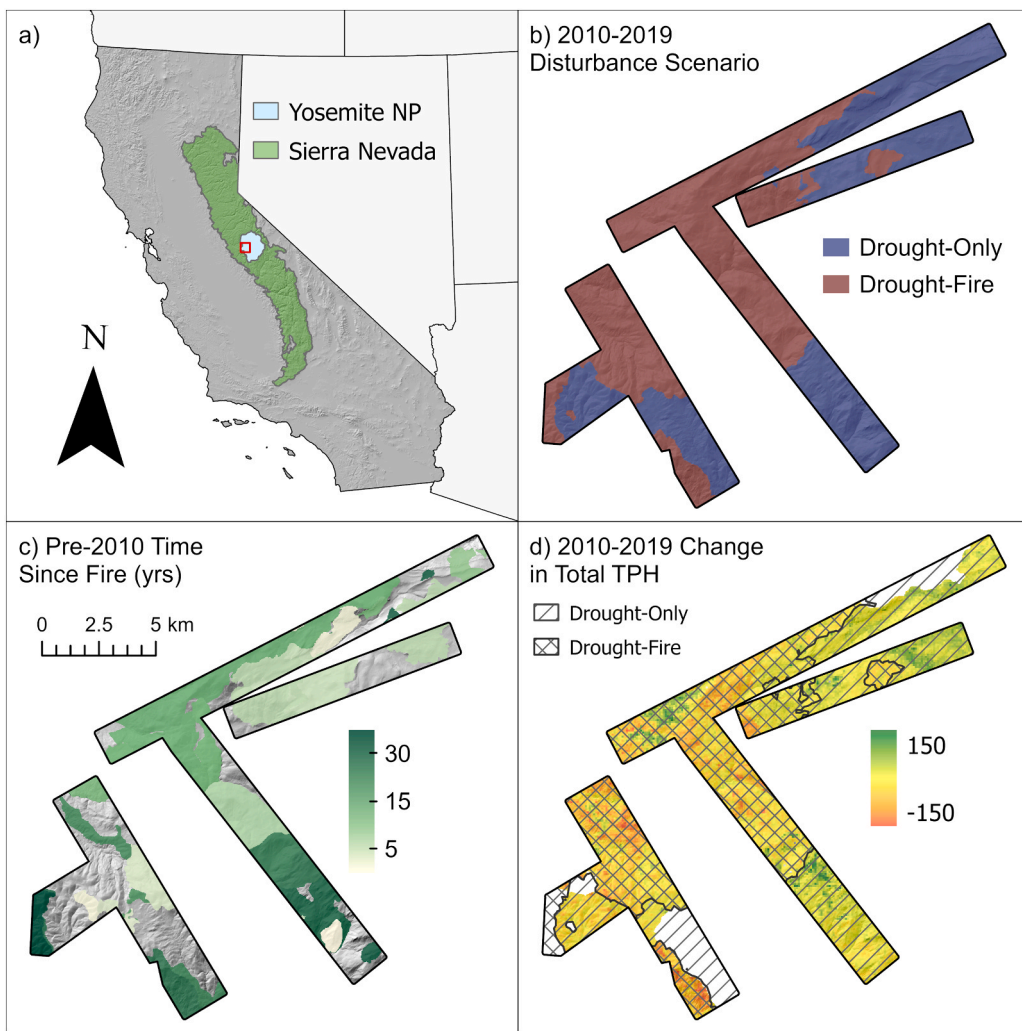


Fig. 1. Study area representing the overlap of the 2010 and 2019 airborne lidar acquisitions within Yosemite National Park, California, USA, with (a) the study area location in California, (b) extent of the drought-only and drought-fire contexts, (c) years since last pre-disturbance fire, and (d) mapped change in total TAO^{-ha} from 2010 to 2019 measured at 90 m resolution. The white area inside the study area boundaries in panel (d) represent masked out sites where a fire burned immediately prior to either the 2010 or 2019 lidar acquisition and thus measures of mortality were not reliable. NP, National Park; TAO, Tree Approximate Object; TPH, TAOs^{-ha}.

1291 mm (Abatzoglou, 2013) and elevation ranges from 1287–2545 m. Within our study area, we constrained our analyses to the historically fire-adapted YPMC forest types (using the FVEG Wildlife Habitat Relationship codes). Dominant tree species within YPMC forests include Jeffrey pine (*Pinus jeffreyi*), ponderosa pine (*Pinus ponderosa*), Douglas-fir (*Pseudotsuga menziesii*), sugar pine (*Pinus lambertiana*), incense-cedar (*Calocedrus decurrens*), and white fir (*Abies concolor*). At lower elevations, *Pinus* species are more common and often intermix with California black oak (*Quercus kelloggii*), while higher elevations tend to have higher proportions of white fir and intermixing components of red fir (*Abies magnifica*) and lodgepole pine (*Pinus contorta* var. *murrayana*) (Safford and Stevens, 2017).

Prior to Euro-American colonization, YPMC forests were characterized by a frequent and low-severity fire regime with an approximate mean fire return interval of 11–16 years (Safford and Stevens, 2017). Wildfires and Indigenous burning practices were excluded from these landscapes for over a century beginning in the mid-1800s and extending to today (Taylor et al., 2016; Klimaszewski-Patterson et al., 2024). However, in Yosemite National Park, fire management policies began to support the reintroduction of low-severity fires as early as the 1960s (van Wagendonk, 2007; Collins and Stephens, 2007), such that many landscapes within the park (including in our study area) have burned once and sometimes multiple times in recent history (Fig. 1c).

Satellite-derived burn severity estimates (Parks et al., 2019) revealed that fires prior to 2010 in our study area resulted in primarily low- and moderate severity effects, with only small patches of high severity (Appendix S1: Figure S1), thus resembling the historical fire regime for these forest types (Safford and Stevens, 2017).

2.2. Defining disturbance contexts

Forests within Yosemite National Park were impacted extensively by the extreme 2012–2016 drought and subsequent bark beetle outbreaks (Hankin et al., 2024). Recent studies indicated that this drought event was the most severe in at least the past 1000 years for the region (Griffin and Anchukaitis, 2014). Considering the pervasiveness of the drought and the often coincident occurrence of drought and bark beetles, we ubiquitously classified *all* sites within our study area as a drought context (Fig. 1b), with this classification serving as an umbrella category to include the impacts of both drought and bark beetles.

Between 2010 and 2019, portions of our study area were impacted by several wildfires including the 2011 Bald and Tamarack fires, the 2013 Rim Fire, the 2014 El Portal Fire, and the 2015 Middle Fire; we classified all these sites as a drought-fire context (including drought-fire and fire-drought sequences) (Fig. 1c). The portions of these fires impacting our study area burned under moderate fire weather

conditions (burning index <80; mapped using the GRIDMET dataset (Abatzoglou, 2013) and the Parks 2014 burn progression layers) and were managed under a range of wildfire management strategies from full suppression to non-full suppression objectives (including resource objectives). Burn indices below 80 are generally associated with flame lengths < 2.4 m and firefighters often use direct attack approaches under these conditions. Lydersen et al. (2014) found that sites within the Rim Fire with burning index < 75 tended to have primarily moderate severity effects on vegetation.

2.3. Measuring structure with airborne lidar

We produced 90-m resolution live-canopy structure metrics from 2010 and 2019 airborne lidar acquisitions. Airborne lidar data was acquired over our study area in July 2010 and October 2019, both during leaf-on conditions. The 2010 survey, conducted with a dual Leica ALS50 Phase II sensor, achieved an average density of 10.9 pulses m^{-2} , while the 2019 survey, conducted with a Riegl VQ-1560i sensor, achieved 23.4 pulses m^{-2} . True-color orthophotos were collected along with the 2010 acquisition using a Leica RCD-105 digital camera, with 15-cm native resolution. Both lidar datasets were processed following American Society for Photogrammetry and Remote Sensing (ASPRS) classification standards. Vertical accuracies (Root Mean Squared Error) of 0.044 m in 2010 and 0.053 m in 2019 were reported, based on 531 and 66 Real-Time Kinematic survey points, respectively. Both acquisitions met the United States Geological Survey's Quality Level 1 standard, suitable for vegetation-related research (Mitchell et al., 2018). Final LAS files, ground models, intensity layers, and ortho imagery for 2010 were obtained from Jim Lutz, at Utah State University (personal communication, 2024), while 2019 products were obtained through the USGS 3DEP program on OpenTopography.

To assess potential influence of differences in pulse density, we conducted a sensitivity analysis by iteratively downsampling the pulse density of the 2019 acquisition, recomputing structure metrics (total TPH and TPH by clump size and height class; see methods below), and plotting the mean and standard deviation of each metric under a range of pulse density scenarios including the 25th percentile, mean, and 75th percentile of the 2010 acquisition. We found that variation in pulse density had minimal effects on structure metrics and therefore on subsequent analyses (Appendix S1: Figure S2). This aligns with past research showing that tree segmentation algorithms perform reliably when pulse density exceeds ~ 8 pulses m^{-2} (Kaartinen et al., 2012; Jeronimo et al., 2018; Sparks et al., 2022).

We used the Forest Service's FUSION software to segment individual trees and to produce canopy height models (CHMs) and intensity rasters from each acquisition (McGaughey, 2020). We refer to lidar-segmented trees as tree approximate objects (TAOs) to acknowledge that lidar-segmented trees often represent a single overstory tree and zero to several subordinate trees (Jeronimo et al., 2018). Prior to producing CHMs and intensity rasters and segmenting TAOs, we normalized each point cloud so that Z coordinates measured vegetation height above ground. To assess potential bias from differences in ground classification, we compared the 2010 and 2019 ground models and found negligible differences (Appendix S1: Figure S3) suggesting that ground model variability was unlikely to affect our results. We produced 0.75-m resolution canopy height models (smoothed using a 3×3 -cell mean filter) from each acquisition and used the watershed algorithm to identify TAO high points and assign segments of the CHM to them. We also produced a corresponding 0.75-m intensity layer representing the mean near infrared reflectance of all points within each cell. For consistency across acquisitions, we assumed circular crowns and estimated crown radius from the area of CHM cells assigned to each high point; this approach allowed us to avoid using FUSION-based crown radii, which in exploratory analyses tended to underestimate crown size.

To quantify live-canopy structure, we trained TAO-level mortality models for each acquisition and excluded predicted-dead TAOs prior to

computing density, clumping, and height metrics (Khatri-Chhetri et al., 2024). To predict TAO-level mortality, we first produced training datasets for each acquisition comprised of 4000 TAOs. The 4000 TAOs were sampled from each acquisition using a stratified random sampling design (stratified by recent disturbance history (Housman et al., 2022), clump size, and mean lidar intensity). Each TAO was labeled live/dead/unknown (see examples in Appendix S1: Figure S4) using RGB orthophotos and 0.75-m lidar intensity (2010 labels derived from 15-cm imagery collected with the lidar and 2019 labels derived from 60-cm NAIP imagery from 2020). We labeled a TAO as live if > 50 % of the crown appeared to be live in the aerial imagery. TAOs for which the imagery did not enable reliable labeling were marked as unknown and discarded from subsequent modeling (3.2 % and 4.8 % of the 2010 and 2019 training datasets, respectively).

We extracted five predictors: mean, minimum, maximum, and standard deviation of lidar intensity within each TAO polygon, and the height to crown area ratio (to help distinguish tall snags with small, dead crowns). Because classes were imbalanced (many more live trees), we balanced training data to equal live/dead counts (final $n = 1416$ and 1464 for 2010 and 2019). We fit RF models using the *tidymodels* (Kuhn and Wickham, 2020) and *ranger* (Marvin and Ziegler, 2017) packages in R, fitting on 75 % of the data and evaluating fit on the remaining 25 %. We provide maps of the training and testing data in Appendix S1: Figure S5, confusion matrices and overall accuracy in Appendix S1: Table S1/S2, and RF variable importance plots in Appendix S1: Figure S6/S7. We evaluated residual spatial autocorrelation across lag distances 90–10,000 m for each model (Appendix S1: Figure S8/S9), and we computed overall accuracy and mean cross-validated accuracy from a spatial cross-validation procedure (Appendix S1: Figure S10/S11) (Ploton et al., 2020). We also computed commission/omission error rates by disturbance scenario and TAO height class for each year (Appendix S1: Figure S12) to contextualize and interpret our modeling results.

After fitting our 2010 and 2019 mortality models, we predicted TAO status across each acquisition and excluded predicted-dead TAOs from subsequent analyses. Because exploratory analyses revealed that mortality models over-predicted live trees in very recent fire areas (red-phase crowns), we masked out locations burned within one year prior to lidar from all subsequent analyses. We note that classification accuracies were relatively high – in 2010, 91.8 % overall accuracy (spatial CV = 92.1 %) with 6 %/12 % commission/omission for dead TAOs and in 2019, 91.9 % overall accuracy (spatial CV = 91.0 %) with 2 %/9 % commission/omission – which generally supports our attribution of density, clump, and height shifts primarily to disturbance-related mortality (though see caveats related to commission and omission errors in results).

From the live TAOs in each acquisition, we produced 90-m resolution rasters of total TAO ha^{-1} as well as metrics quantifying the proportion of total tree density represented by different TAO clump sizes and height classes (i.e., “proportion metrics”). We computed all structure metrics at a 90-m spatial resolution since past work indicates that fine-scale tree clump and opening patterns tend to emerge at approximately this scale in frequent-fire forests under active fire conditions (Larson and Churchill, 2012) and to align with related studies (e.g., Pawlikowski et al., 2019). For the tree clumping algorithm, “TAO A” was considered clumped with “TAO B” if the inter-tree distance was less than the sum of TAO crown radii (based on circular estimates of TAO crowns), and clump membership percolated such that any other TAOs clumped to “TAO B” were also considered clumped with “TAO A”. Each TAO’s clump size was equal to the number of TAOs in its clump. We classified clumps as 1–4, 5–9, and 10-plus to support comparison with related studies (Lydersen et al., 2013; Kane et al., 2019) and TAO heights as 2–16 m, 17–32 m, and 32 m plus to support comparison with other related studies (Kane et al., 2014, 2019). Change rasters were computed as 2019 minus 2010 for all metrics (change in total TPH mapped in Fig. 1d).

2.4. Mapping biophysical conditions and fire history

We compiled a variety of predictors to describe environmental conditions in, or prior to, 2010 to use in our drivers of change models. For climate, we used layers from the Basin Characterization Model dataset describing long-term (1981–2010) mean annual actual evapotranspiration (AET, a productivity proxy) and climatic water deficit (CWD, a vegetation stress proxy) (Stephenson, 1998; Flint et al., 2021). For topography, we quantified topographic position index (TPI, a continuous metric differentiating valleys, slopes, and ridges (Jenness, 2007)) and the solar radiation aspect index (SRI, a continuous index differentiating north- and northeast-facing slopes from south and southwest-facing slopes (Roberts and Cooper, 1989)). We quantified TPI using a 510-m moving window since initial results showed that this scale had the strongest relationship with our structural change metrics. For 2010 canopy structure conditions, we used the 2010 lidar data to derive 90-m resolution canopy cover of live TAOs and relative canopy cover in the 2–8 m height strata (a proxy for ladder fuel density) (Hankin and Anderson, 2022; Chamberlain et al., 2024).

We mapped pre-2010 fire history using CALFIRE's Fire and Resource Assessment Program (FRAP) fire history dataset, which included all recorded wildfire and prescribed fire perimeters > 4 ha (FRAP, 2021). We validated records in this dataset against Yosemite National Park fire records. We only included fires that burned 1985–2009 so that Landsat imagery could be used to map burn severity. All areas with fire records prior to 1985 were masked out from subsequent analyses (8 % of the total study area). We produced two fire history datasets: (1) time since fire and (2) most recent burn severity. Maps of these variables are shown in Fig. 1c and Appendix S1: Figure S1, respectively. Time since fire was calculated as the time between the 2010–2019 disturbance and the most recent pre-2010 fire. The 2010–2019 disturbance date was set as either the year of the fire that burned 2010–2019 or as 2012 corresponding with the start of the 4-year drought for the drought-only context. We classified the time since fire as 1–15, 16–30, or ≥ 31 years. We calculated most recent burn severity as the severity of the most recent pre-2010 fire. We used the Google Earth Engine code described in Parks et al. (2019) to map the bias-corrected Composite Burn Index (CBI) (Key and Benson, 2006) at 30-m resolution for all pre-2010 fires, then created a composite layer representing the most recent CBI value.

2.5. Statistical analyses

To assess how tree density, clumping patterns, and height distributions changed in the drought-only and drought-fire context, we first plotted TAO height distributions for each height class for all TAOs and for TAOs belonging to each clump size in 2010 and 2019 (we also provide continuous distributions of height by clump class in Appendix S1: Figure S13).

We then fit a series of models to assess (1) how tree density, proportion of TAOs in each clump class, and proportion of TAOs in each height class changed in the drought-only and drought-fire context and (2) how pre-disturbance fire history, biophysical setting, and forest structural patterns influenced patterns of structural change. Prior to modeling, we reduced predictor multicollinearity and model residual spatial autocorrelation (SA). To reduce multicollinearity, we computed Spearman's correlation coefficient among continuous predictor variables. When correlation among variables exceeded 0.5, we retained the variable yielding the best generalized additive model (GAM) predicting change in total TAO density, with model performance based on the generalized cross-validation score (Wood, 2017). From this process, we included CWD, TPI, SRI, and 2010 total canopy cover, plus the categorical time since fire metric, as predictors in our subsequent models.

To identify a minimum sampling distance, we assessed SA of model residuals using Moran's I statistic. We fit a GAM predicting total change in TPH as a function of the selected environmental variables. We then computed Moran's I of the model residuals at varying lag distances using

the R *ncf* package (Bjornstad, 2022). We found that Moran's I values remained below 0.3 at lag distances greater than 410 m. We therefore used a 450-m minimum among-sample distance (five 90-m cells) to limit SA while maintaining adequate sample sizes.

To quantify the magnitude and direction of change in each structure metric in each disturbance context (drought-only and drought-fire), we fit linear models (Gaussian distribution) for total TAO density and GLMs (beta distribution with a logit link) for proportional metrics (Faraway, 2015), with predictors year, CWD, TPI, and SRI (hereafter "change models"). For proportion metrics, we reclassified all 0's as 0.001 and all 1's as 0.999 to meet the specifications of the beta distribution. We compared fitted means of each metric between 2010 and 2019 in each disturbance context and assessed 95 % confidence intervals (CIs) around predictions, denoting a significant difference when CIs did not overlap. We used 5-fold CV and report overall R^2 and mean CV- R^2 (Table 1). We plotted raw density curves of each metric to visualize differences between the years in each disturbance context. We compared distributions between 2010 and 2019 for absolute values of TPH by clump size and height class membership in Appendix S1: Figure S14.

To quantify drivers of change in each structure metric, we fit GAMs with predictors CWD, TPI, SRI, time since most recent fire, and 2010 canopy cover (hereafter "drivers of change models") (Wood, 2017). Samples with zero 2010 structure for the focal metric were excluded so "no change" reflected loss/gain of existing structure. We assumed a Gaussian error distribution (validated post-hoc). We fit time since fire as a linear predictor and fit each continuous predictor using thin plate regression splines with a basis dimension of 5. We set the parameter "select" as "true" and used a gamma value of 1.4 to allow moderate penalization terms in each model, which allowed fitting of non-linear, linear, and 0 coefficients (Marra and Wood, 2011; Wood, 2017). To plot fitted relationships, we predicted the mean and 95 % CIs of each metric across the full range of each environmental variable, while holding other variables at their means. For predictions of continuous variables, we set time since fire as 15–30 years as a surrogate for the mean time since pre-disturbance fire in our study area. We used 5-fold CV and report overall R^2 and mean CV- R^2 (Table 1). We provide modeled predictions across environmental variables for absolute change in TPH by clump size and height class membership in Appendix S1: Figure S15/S16.

3. Results

3.1. Changes in structure through drought-only and drought-fire

In the drought-only context, total TPH increased by 10 % between 2010 and 2019 (Fig. 2), with increases interpreted as ingrowth or canopy exposure and decreases as mortality. Of this change, short (2–16 m) and medium (17–32 m) TAOs increased by 33 % and 2 %, respectively, while tall (32 m +) TAOs declined by 5 % (Fig. 2a). All clump sizes experienced similar height class changes, with the most notable increases in short (2–16 m) TAOs belonging to small, medium, and large clumps (Fig. 2b-d). Omission exceeded commission errors for medium (7.4 %) and tall (14.5 %) TAOs in 2010, and for short (10.4 %) and tall (7.2 %) TAOs in 2019. These imbalances suggest that some apparent ingrowth of short TAOs in the drought-only context may reflect misclassification of live TAOs in 2019, while losses of tall TAOs may be overestimated due to the overclassification of live TAOs in 2010 for tall TAOs (Appendix S1: Figure S12).

In the drought-fire context, total TPH declined by 25 % from 2010 to 2019, with a 28 % increase in short TAOs and 50 % and 35 % reductions in medium and tall TAOs, respectively (Fig. 2e). Losses were concentrated in large clumps, with reductions of 74 % and 62 % of medium and tall TAOs, respectively (Fig. 2h). In contrast, medium and tall TAOs in small and medium clumps remained stable or slightly increased in the drought-fire context (Fig. 2f-g). Omission exceeded commission errors (4.6 %) in 2019 for the drought-fire context, suggesting that reductions

Table 1

Descriptions and performance statistics for 14 change models and 14 drivers of change models. CV: cross validation; GLM: generalized linear model; CWD: climatic water deficit; TPI: topographic position index; SRI: solar radiation index; TAO: tree approximate object; TPH: TAOs per hectare; GAM: generalized additive model; CC: canopy cover; TSF: time since fire; pSmC: proportion small clump; pMdC: proportion medium clump; pLgC: proportion large clump; pShT: proportion short TAOs; pMdT: proportion medium TAOs; and pTIT: proportion tall TAOs.

Model Category	Model Type	Predictors	Error Dist.	Response	Drought-Only ($R^2/CV R^2$)	Drought-Fire ($R^2/CV R^2$)
Change	Linear GLM	Year, CWD, TPI, SRI	Gaussian Beta	TPH	0.18/0.08	0.14/0.11
Drivers of Change	GAM	2010 CC, CWD, TPI, SRI, TSF	Gaussian	pSmC pMdC pLgC pShT pMdT pTIT Δ TPH Δ pSmC Δ pMdC Δ pLgC Δ pShT Δ pMdT Δ pTIT	0.14/0.07 0.08/-0.02 0.11/0.04 0.18/0.15 0.04/-0.03 0.33/0.22 0.50/0.31 0.41/0.26 0.17/-0.22 0.45/0.20 0.14/-0.00 0.26/0.04 0.06/-0.19	0.17/0.16 0.08/0.02 0.20/0.24 0.10/-0.03 0.10/0.05 0.05/-0.03 0.41/0.33 0.39/0.35 0.19/0.04 0.40/0.32 0.17/0.09 0.13/0.02 0.09/0.05

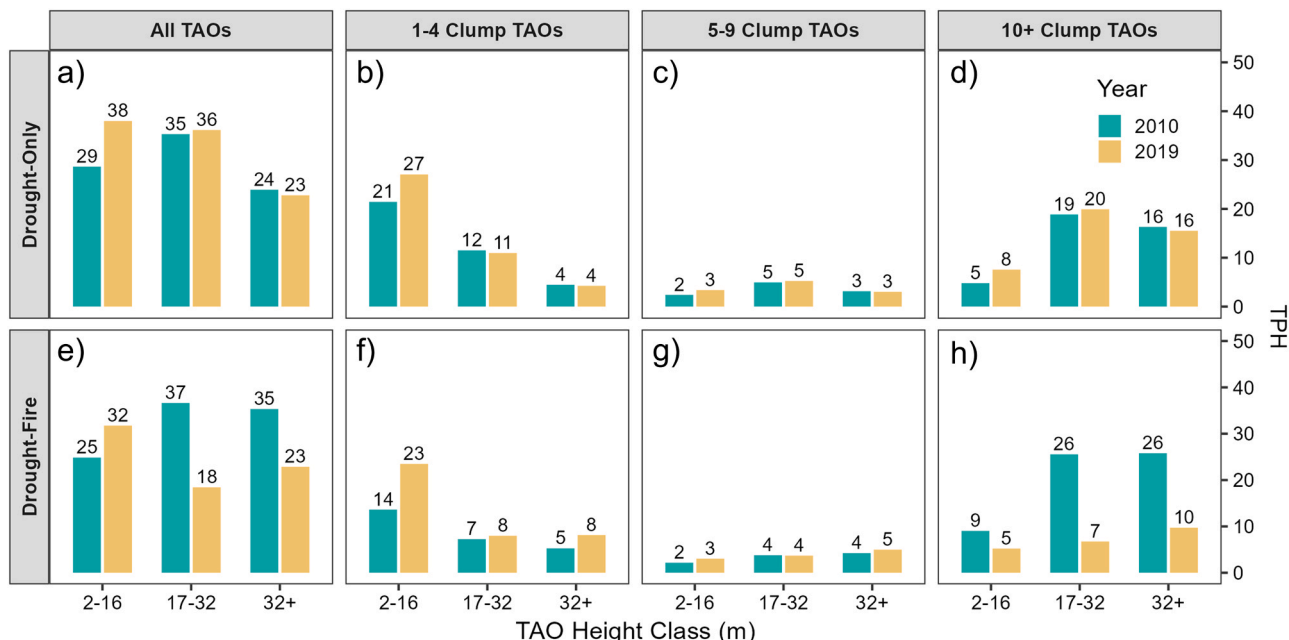


Fig. 2. Comparisons of TAO^{ha} (TPH) between 2010 and 2019 by height class and clump size membership for the (a-d) drought-only and (e-h) drought-fire contexts in active-fire landscapes within Yosemite National Park, California, USA.

in TPH may be underestimated due to overclassification of live TAOs in 2019. Also, similar to the drought-only scenario, some of the apparent ingrowth of short TAOs may be overestimated due to the overclassification of live TAOs in 2019.

For drought-only change models, mean CV- R^2 values were low (<0.23, Table 1), and model-predicted means across structure metrics showed negligible, non-significant differences (Fig. 3a). Distributional shifts between 2010 and 2019 (i.e., Fig. 3 violin plots) generally mirrored these results, with moderate increases in total TPH and proportional increases in large clump membership and short TAOs (Fig. 3a).

Structural change was greater in the drought-fire context, where models indicated decreased TAO density and a shift toward more open structural conditions (Fig. 3). Mean CV- R^2 exceeded 0.1 for models of total TPH, small clump, and large clump proportions (Table 1), which also showed the largest and significant changes. Total TPH decreased by 24.8 (from 102.0 to 77.2) from 2010 to 2019 (though we note that this loss may be underestimated due to misclassification of live TAOs in 2019). TPH distributions shifted toward lower post-disturbance

densities, yet most sites maintained TPH values > 25 (Fig. 3b). We observed a 0.26 increase in the proportion of small clump membership and a 0.23 decrease in the proportion of large clump membership from 2010 to 2019 (Fig. 3b), while medium clump membership showed negligible change ($CV-R^2 = 0.02$). We observed a 0.13 and 0.15 proportional increase of short and medium TAOs, respectively, and a 0.06 proportional decrease of tall TAOs (Fig. 3b), though $CV-R^2$ for these models was low (<0.05, Table 1). Distributional shifts generally showed stability of small clumps and decreases in large clumps (Fig. 3b).

3.2. Drivers of change during drought-only and drought-fire

CV- R^2 values from drought-only drivers-of-change models were generally higher than from drought-only change models but remained ≤ 0 for models predicting change in the proportion of medium clumps, short TAOs, and tall TAOs. We therefore refrain from extensive interpretation where model performance was poor. Overall, results indicated that pre-drought canopy cover, biophysical setting, and pre-2010 fire

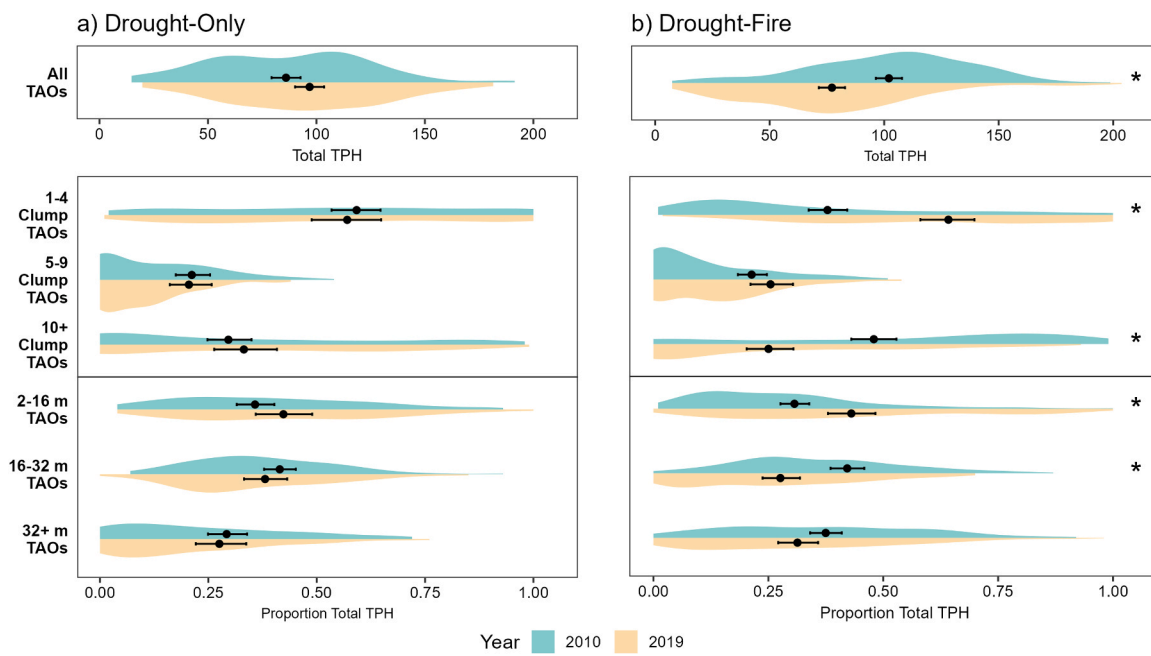


Fig. 3. Differences between 2010 and 2019 for total TAO ha^{-1} (TPH), and proportion of TPH by TAO clump size and height class in the (a) drought-only and (b) drought-fire contexts, for active-fire landscapes within Yosemite National Park, California, USA. Density distributions represent all sample points. Points and error bars show model-predicted means and 95 % confidence intervals, respectively, from linear models (All TAOs) and generalized linear models (clumping and height metrics). Asterisks (*) indicate non-overlapping confidence intervals.

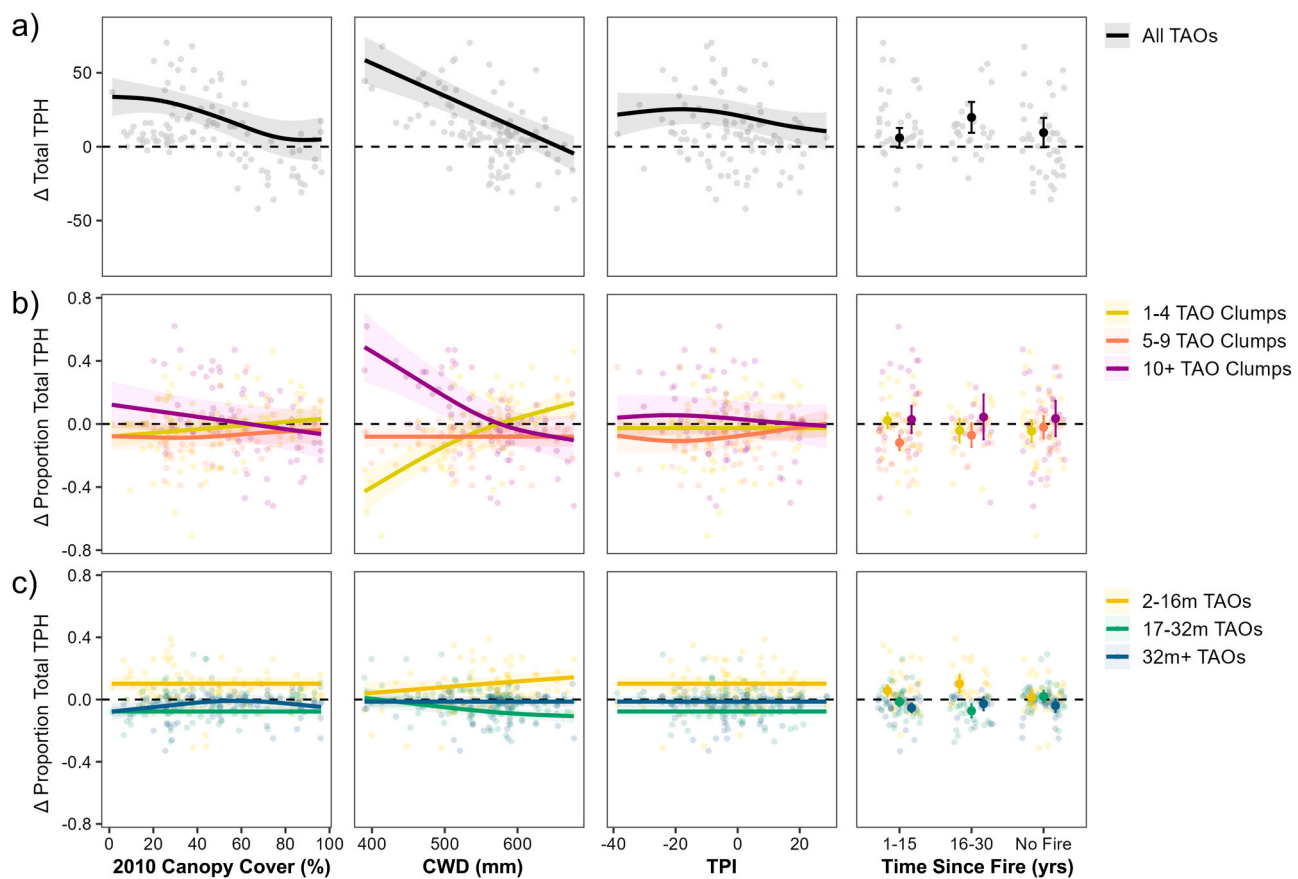


Fig. 4. Fitted relationships between environmental variables and changes in (a) total TPH and proportion of total TPH by (b) tree clump membership and (c) height class, for the drought-only context in active-fire landscapes within Yosemite National Park, California, USA. In the left three columns, lines represent model estimates (holding all other predictors at their means), and shaded regions represent 95 % confidence intervals. In the rightmost column, full color points and error bars show model estimates (holding all other predictors at their means) and 95 % confidence intervals, respectively. Transparent background points show the distributions of sample points in each model.

history had only moderate impact on structural change in the drought-only context (Fig. 4). Increases in total TPH (likely overestimated due to misclassifications in the mortality models) were associated primarily with locations where 2010 canopy cover was lower (<60 %) and in more moist climatic settings (CWD <500 mm). Topographic position and fire history were less influential, though less exposed topographic positions (TPI <0) and sites that had experienced fire 16–30 years prior to the drought showed slight increases in TPH (Fig. 5a). The largest shifts in clump membership were observed at CWD < 500 mm and, to a lesser extent, when 2010 canopy cover was < 20 %, where a ~0.40 decrease in small clumps corresponded with a ~0.40 increase in large clumps (Fig. 4b). Height class changes showed only subtle trends across environmental gradients in the drought-only context (Fig. 4c); irrespective of 2010 canopy cover and topographic positions, short TAOs increased by ~0.10 while medium and tall TAOs declined by ~0.10 and ~0.05, respectively. Losses of medium and tall TAOs were slightly greater under more climatically stressed (higher CWD) conditions (Fig. 4c).

In the drought-fire context, changes in total TPH and TAO clumping patterns were moderately influenced by 2010 total canopy cover and TPI (Fig. 5). All models had $CV-R^2 > 0$, though those predicting medium clumps and height classes were still relatively low (0.02–0.09), indicating that pre-disturbance canopy cover, topographic position, and fire history best explained changes in total TPH and clump membership. As 2010 canopy cover increased and topographic position transitioned from valleys to ridges, combined drought and fire effects resulted in greater loss of total TPH (Fig. 5a) (though these losses may be somewhat underestimated due to misclassification of live TAOs in 2019). Reductions in TPH were associated almost exclusively with declines in

large clumps (up to 0.80) and increases in small clumps (up to 0.45), indicating a disaggregation of larger clumps when 2010 canopy cover was higher and in more exposed topographic positions (Fig. 5b). Time since fire had no significant effect on TPH change (though a non-significant trend of increasing loss with longer time since fire was observed), but it did affect TAO clump membership: sites with no fire history showed stronger shifts from large to small clumps than sites that burned within the past 30 years (Fig. 5b). Changes in height distributions were less effected by environmental gradients (Fig. 5c), with all sites showing a ~0.20 increase in short TAOs, and ~0.10 and ~0.05 decreases in medium and tall TAOs, respectively. This pattern was slightly stronger in sites with > 80 % canopy cover, in valleys, and when time since fire was 16–30 years (Fig. 5c).

4. Discussion

Our results indicate that reintroducing a frequent, low- to moderate-severity fire regime to fire-adapted dry forest ecosystems can promote stability in key forest structural patterns (e.g., tree density, height distributions, and clumping patterns) and enhance ecological resilience. Within the active-fire landscapes in our study area, tall TAOs and small TAO clumps persisted as consistent structural features even under the combined pressures of extreme drought and moderate-intensity fire, whereas large TAO clumps were less stable, tending to disaggregate into smaller clumps. Where structural changes did occur, they were not random, but instead reflected gradients of pre-disturbance canopy cover, topographic position, and the timing of past fires, suggesting that fine-scale biophysical and disturbance history gradients drive structural

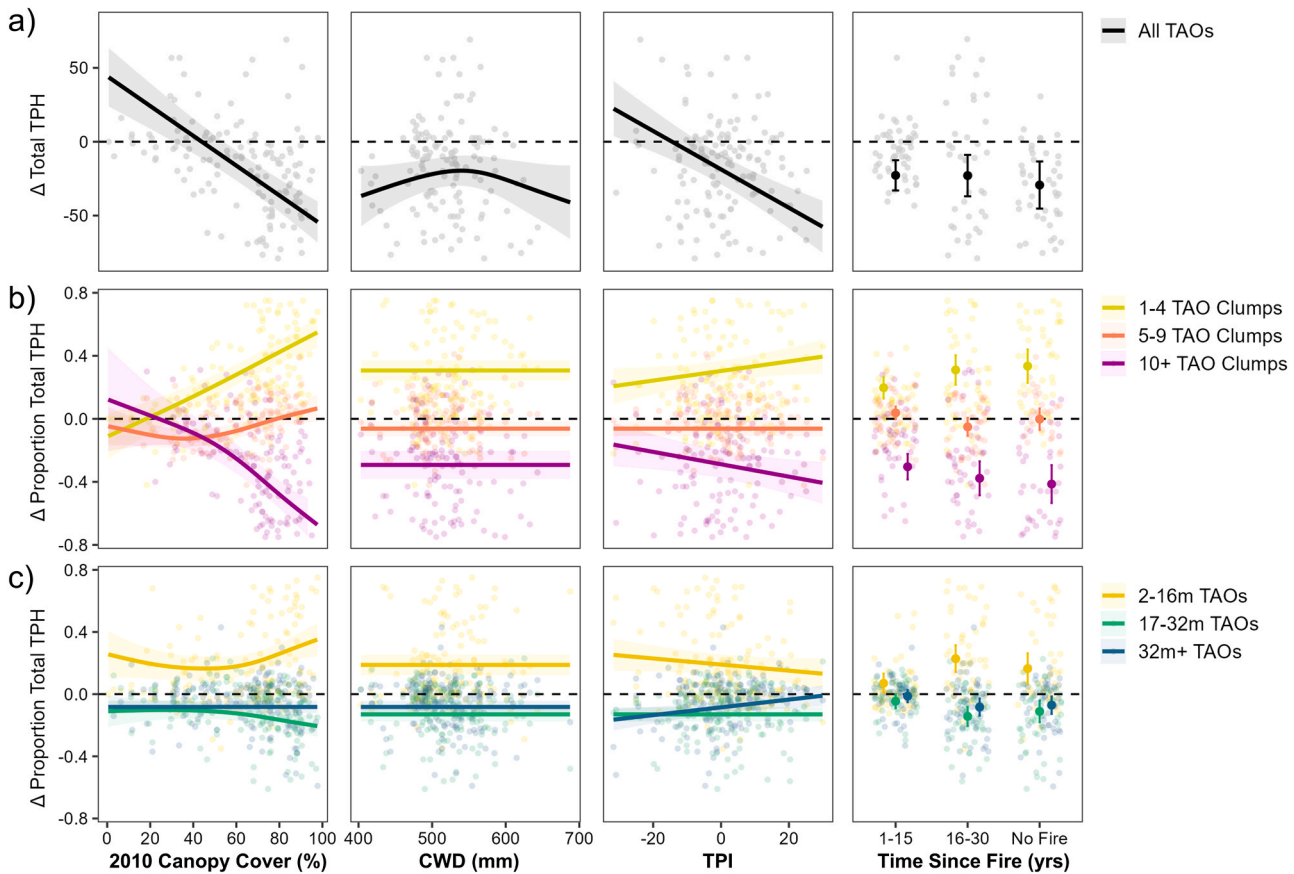


Fig. 5. Fitted relationships between environmental variables and changes in (a) total TPH and proportion of total TPH by (b) tree clump membership and (c) height class, for the drought-fire context in active-fire landscapes within Yosemite National Park, California, USA. In the left three columns, lines represent model estimates (holding all other predictors at their means), and shaded regions represent 95 % confidence intervals. In the rightmost column, full color points and error bars show model estimates (holding all other predictors at their means) and 95 % confidence intervals, respectively. Transparent background points show the distributions of sample points in each model.

changes in active-fire landscapes (Fig. 6; Appendix S1: Figure S16/S17). Our study underscores the ecological value of restoring active-fire conditions in fire-adapted ecosystems, especially in an era marked by rapid environmental change.

4.1. Active-fire landscapes demonstrate resistance to drought

We observed a moderate degree of structural resistance in the mid and upper canopy during the severe 2012–2016 drought in our study. While we did observe an approximate 5 % loss of tall trees – which may be of management relevance in many cases – our results largely contrast with the much higher mortality reported at lower elevations in the south and central Sierra Nevada during the drought (Young et al., 2017; Fettig et al., 2019; Restaino et al., 2019). Our results do, however, generally align with other work from the mid- to upper-montane zone and especially within partially restored active-fire landscapes (Boisramé et al., 2017; Murphy et al., 2021; Furniss et al., 2022).

We posit that the moderate structural resistance observed within our study area in the drought-only context reflected (1) the site's higher elevation and thus relatively wetter conditions and (2) the reduced pre-drought local tree densities resulting from recent active-fire management (Fig. 3; Hood et al., 2015; Willson et al., 2024). Indeed, past work

shows that higher elevations in the Sierra Nevada mixed-conifer zone were characterized by relatively higher precipitation and lower climatic water deficit during the drought (Young et al., 2017), which tended to promote overall tree health and increase tree-level defense mechanisms (Fettig et al., 2019; Restaino et al., 2019). Additionally, past work showed that sites with reduced local tree densities, and thus reduced inter-tree competition, resulting from past fire or other management, exhibited lower drought-related mortality (Young et al., 2017; Furniss et al., 2020, 2022). Importantly however, we acknowledge the limitations of a strictly airborne lidar-based study, which limited our ability to characterize sub-canopy mortality rates; thus, our results may be biased toward lower mortality estimates compared to field-based studies (e.g., see Hankin et al., 2024). Additionally, some of the apparent increase in short TAOs in the drought-only context may reflect higher omission error in the 2019 mortality classification (Appendix S1: Figure S12) or the release of previously occluded understory trees that became detectable following overstory mortality. Thus, results regarding increases in short TAOs in the drought-only context should be interpreted with caution.

The drought-only affected portion of our study area was characterized by relatively high variability in structural conditions in 2010 (i.e., a wide distribution of total TPH in 2010; Fig. 3a), suggesting increased

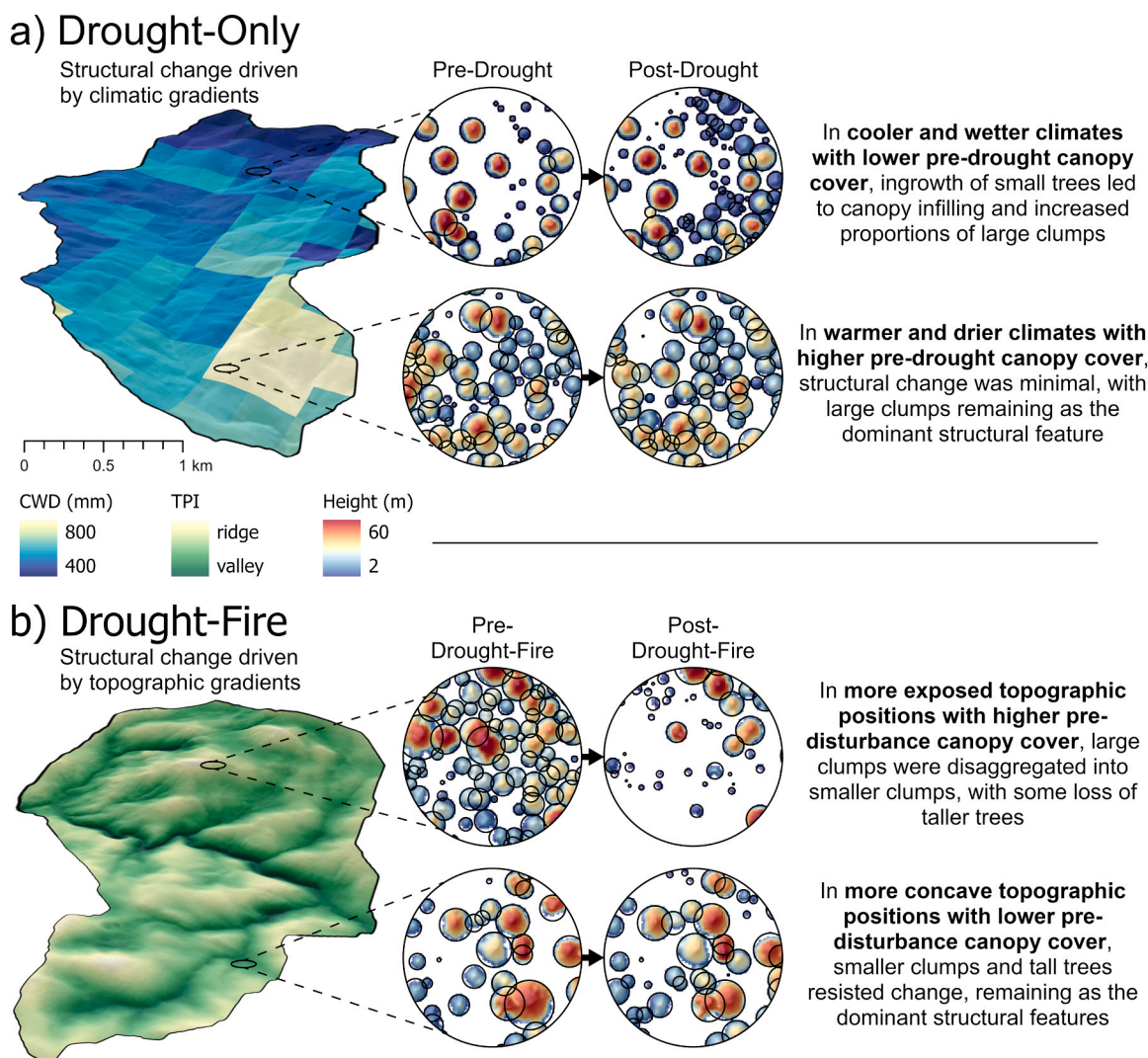


Fig. 6. Conceptual diagram illustrating structural dynamics in an active-fire dry forest landscape under (a) drought-only and (b) drought-fire contexts. Circular insets (~ 0.5 ha) show how shifts in TAO spatial patterns and height distributions from 2010 to 2019 vary across a gradient of climatic water deficit (a, drought-only context) and a gradient of topographic position index (b, drought-fire context).

landscape-level heterogeneity likely due to the history of active-fire management (Fig. 3a). We believe that this heterogeneity may have further enhanced neighborhood-level resistance of TAOs. Heterogeneous structural patterns are associated with more diverse species assemblages and more discontinuous canopies, both of which can inhibit the growth and spread of bark beetle populations and reduce subsequent severity (Fettig et al., 2007; Turner et al., 2013; Hessburg et al., 2019; Restaino et al., 2019; Koontz et al., 2021). Our results provide evidence that the landscape heterogeneity produced by an active-fire regime (Collins et al., 2016; Chamberlain et al., 2023a) may contribute to increased tree- and neighborhood-level structural resistance during periods of intense drought.

4.2. Tall tree and small clump resistance during drought-fire

Our study showed that key structural features – those which define fine-scale structural patterns in fire-adapted dry forest ecosystems (Larson and Churchill, 2012; Lydersen et al., 2013) – exhibited stability at landscape scales during fire and drought. In particular, TAOs belonging to small- and medium-sized clumps persisted in relatively constant densities, and tall TAOs showed reasonably high stability in both their proportions and counts (Fig. 2f–g; Fig. 3b). This apparent stability of small clumps may reflect both the resistance of pre-fire small clumps and the disaggregation of larger clumps into smaller clumps during fire. The persistence of these backbone structural features will promote continued resistance, and likely resilience and adaptability, of these forests under changing climatic conditions (Stephens et al., 2008; Churchill et al., 2013; Koontz et al., 2020; Ziegler et al., 2021; Falk et al., 2022). Past work has primarily documented subsequent burn severity patterns in active-fire landscapes, showing a tendency toward lower burn severities (Lydersen et al., 2014; Kane et al., 2015a). This study provides additional insight at a much finer-spatial scale, showing that low- and moderate-severity fire effects in active-fire landscapes reflect stable patterns of small and medium sized TAO clumps and high proportions of tall TAOs.

Importantly, we note that the portions of fires that impacted our study area from 2010 to 2019 all burned under low and moderate fire weather conditions (burning index <80). As such, our work highlights the beneficial role that fires can play during non-extreme burning conditions and emphasizes an urgent need to diverge from suppression-focused policies so that more fires can burn under these more moderate fire weather conditions (North et al., 2021, 2024). Future research can build on existing work (e.g., Lydersen et al., 2014; Steel et al., 2021a; 2023) to better define thresholds and tipping-points of structural resistance in active-fire landscapes under a wider range of fire weather and climate scenarios.

Even within the context of active-fire landscapes, our results show that tall trees within large clumps were highly susceptible to loss during drought and fire (e.g., a 62 % reduction of >32 m TAOs that belonged to large TAO clumps in the drought-fire context) (Fig. 2h). Tall and large trees are critical backbones of forest structure in dry forest ecosystems and contribute disproportionately to carbon storage and regulation of ecological processes (Lutz et al., 2012; Hessburg et al., 2015). Tall trees are also important habitat features for the California spotted owl (*Strix occidentalis occidentalis*) and fisher (*Pekania pennanti*) (North et al., 2017; Blomdahl et al., 2019; Kramer et al., 2021). Moreover, recent work by Kane et al. (2023) showed that a majority of the tall and very tall trees across the Sierra Nevada exist in locally-dense, closed-canopy forest conditions. If a management objective is to conserve tall trees in Sierra Nevada YPMC forests, we suggest that efforts focus on creating or reinforcing fine-scale patterns of small and medium-sized clumps across the landscape (Churchill et al., 2013; Kane et al., 2019). As shown in Fig. 2f and Fig. 2h, post-drought-fire landscapes retained nearly the same density of tall TAOs in small clumps as in large clumps (8 vs. 10 TPH), underscoring that management emphasizing smaller clump sizes can sustain relatively high densities of tall trees.

The stability of small clumps through drought and fire in our study may be due to two complementary mechanisms. First, it is likely that pre-fire small clumps were more resistant to loss due to their inherent structural properties and influence on fire behavior. Recent fire behavior modeling studies have shown that individual trees and small clumps are less susceptible to crown fire due to convective cooling around smaller clumps (Ritter et al., 2020) and more variable surface wind patterns produced by heterogeneous fuel structures (Atchley et al., 2021). Our results support these studies and provide empirical evidence of small clump resistance in contemporary active-fire landscapes (Fig. 2f–g; Fig. 3b; Pawlikowski et al., 2019). Second, because the fires that affected our study area all burned under non-extreme fire weather conditions, it is likely that the stability of small clumps across the landscape was in part due to the disaggregation of large clumps into smaller clumps during fire, which is consistent with past work showing the disaggregating effect of fires that burn during non-extreme weather conditions (Kane et al., 2013, 2019; 2014). Together, these processes likely contributed to the stability of small- and medium-sized clumps in our study.

4.3. Biophysical drivers of structural change and heterogeneity

We found that biophysical gradients had a relatively strong influence on patterns of structural change in the drought-fire context (Fig. 5). Across all biophysical gradients, we observed a disaggregation of larger clumps into smaller clumps (similar to findings from Kane et al. 2013; 2014) (Fig. 3b). Importantly however, these patterns were accentuated in areas with higher pre-fire canopy cover, in more topographically exposed sites, and when time since fire was longer. Past work has documented that fine-scale forest structural patterns tend to align with topographic gradients in the Sierra Nevada (i.e., higher density conditions in valleys and more open-canopy conditions on ridges) (Lydersen and North, 2012; Jeronimo et al., 2019; Ng et al., 2020). Our explicit tracking of structural conditions through time suggests that these topographically-mediated structural patterns are more than simply a reflection of topographic influences on resource gradients, but that they also reflect how these resource gradients influence fire behavior (and drought effects) which in turn influence structural conditions and dynamics (Lydersen and North, 2012; Kane et al., 2015b).

4.4. Implications of field-based studies

While airborne lidar affords many advantages in terms of quantifying forest structural patterns, a key weakness is its capacity to identify and measure tree species compositions (Jeronimo et al., 2018). Several field-based studies evaluating plot-level mortality during the 2012–2016 drought indicated much higher mortality for *Pinus* species, particularly at lower elevations (Fettig et al., 2019; Steel et al., 2021b; Das et al., 2022). Additionally, several studies showed that conspecific tree density had a strong positive influence on mortality for individual tree species (Restaino et al., 2019; Furniss et al., 2022; Germain and Lutz, 2024). During drought in our study, we observed a slight but non-significant decrease in the proportion of large TAOs (Fig. 3a), and a slight reduction in the total counts of > 32 m TAOs belonging to large clumps (Fig. 2d). Inferring from field-based studies, we suspect that reported reductions in tall trees in our study primarily reflect losses of *Pinus* species, especially at lower elevations (Fig. 1d) and when they belonged to large clumps with high conspecific densities.

Tree species compositions also have important implications for fire resistance and recovery in YPMC forests (Lydersen et al., 2014; Collins et al., 2018; Germain and Lutz, 2024). Recent work indicates that even after the reintroduction of fire in previously fire-suppressed forests, the proportions of fire-resistant pines may not align with historical estimates (May et al., 2023; Zald et al., 2024). In the context of our study, it is possible that the small and medium clumps and tall TAOs that resisted drought and fire (Fig. 2f–g) were characterized by relatively high

proportions of white fir, a species that generally lacks the fire tolerance of pines (Cansler et al., 2020; Safford and Stevens, 2017). If so, and if pine prevalence is indeed a stronger driver of resistance than structural conditions alone, the active-fire landscapes in our study area may not be fully resistant under futures characterized by increased fire activity (May et al., 2023; Zald et al., 2024). Future work can therefore build on our structure-focused study to better quantify and monitor species-level resistance in active-fire landscapes of the Sierra Nevada (e.g., Blackburn et al., 2025).

Another key limitation of airborne lidar is its inability to characterize surface fuel conditions which, similar to species, have important implications for fire resistance. While recent burning has shown to reduce surface fuel loading in fire-suppressed forests (Cansler et al., 2019; Hankin et al., 2024), drought and bark beetle attacks may counteract these reductions (Reed et al., 2023; Vilanova et al., 2023) and contribute to increased risk to subsequent fires (Hurteau et al., 2024). Future work can evaluate shifts in surface fuel loading where disturbances interact with partially-restored active-fire landscapes, and assess how these dynamics, coupled with overstory conditions, influence resistance and resilience.

4.5. Management implications

While the management history of Yosemite National Park is somewhat unique compared to adjacent private and Forest Service lands (i.e., relative lack of early century logging and early re-establishment of prescribed burning programs) (van Wagtendonk, 2007; Kane et al., 2023), we argue that the active-fire conditions in Yosemite, and their demonstrated resistance, are achievable across other forest landscapes of the Sierra Nevada and western North America. We suggest that managers can increase the extent of active-fire landscapes by:

- (1) Continued implementation of mechanical thinning and prescribed burning programs (North et al., 2021; Davis et al., 2024) particularly in strategic locations that increase the scale of forest restoration (North et al., 2021) and where first-entry fires are *least* likely to achieve restoration targets (e.g., lower elevation yellow pine forests in the northern Sierra Nevada (see Chamberlain et al., 2024))
- (2) Shifting away from strict suppression-focused fire management to allow more low-intensity fires to burn during periods of less extreme weather (North et al., 2021, 2024; Kreider et al., 2024) particularly where first-entry fires are *most* likely to achieve forest restoration targets (e.g., in higher elevation dry mixed conifer forests in the Sierra Nevada and in landscapes with more extensive mosaics of recent fires (see Chamberlain et al., 2024))
- (3) Leveraging the beneficial work of recent fires by implementing ecologically-informed post-fire management strategies, such as strategic mechanical thinning or prescribed burning to maintain resilient structural conditions in patches of low and moderate severity effects (Meyer et al., 2021; Stevens et al., 2021; Larson et al., 2022).

Our results highlight the importance of maintenance burning and/or mechanical treatments in active-fire landscapes. During drought, our results showed increases in total TPH between 2010 and 2019 with a marked increase in the shortest TAOs and a “closing in” of canopy conditions (Fig. 3a; Fig. 4). As such, in drought-affected sites where fires have been absent for more than approximately 15 years, managers may need to prioritize near-term application of prescribed burning, restoration thinning, or managed wildfire to maintain lower tree densities and ensure continued resistance of key structural features. Restoring and maintaining active-fire landscapes is an ongoing process that will require continued input of financial and personnel resources to ensure continued occurrence of frequent and low-severity fires (North et al., 2021, 2024; Hessburg et al., 2021).

Our finding that topography influences patterns of structural change supports common dry forest restoration guidelines in the Sierra Nevada (North et al., 2009). Topography is a key driver of stand-level structural conditions in dry forest landscapes (Lydersen and North, 2012; Ng et al., 2020). Thus, scientists recommend that restoration treatments mirror this underlying topographic template, which can promote landscape heterogeneity and increase the range of management objectives that restored dry forest landscapes achieve (North et al., 2009; Hessburg et al., 2015). Our results extend this concept and show that topographic features also influence patterns of drought- and fire-induced structural change in active-fire landscapes (Fig. 5). As such, we suggest that topographic features continue to inform the design, placement, and prioritization of individual treatments (North et al., 2009) as well as the more comprehensive treatment programs which will dictate how forest ecosystems adapt and change over longer time periods (Hood et al., 2022).

Our results suggest that tall trees (>32 m) exhibited relatively high resistance to drought and fire when they existed within heterogeneous active-fire landscapes. Therefore, if the objective is to conserve tall trees, management can work to restore active-fire conditions, fine-scale tree clump and opening patterns, and landscape-level structural heterogeneity (North et al., 2009; Churchill et al., 2013; Hessburg et al., 2015). However, our results also suggest that losing some tall trees is an inevitable outcome of restoring fire to fire-adapted forests. This suggests a tradeoff in which the landscape benefits achieved by restoring active-fire conditions (e.g., increased resilience, adaptive capacity, wildlife habitat) may come with the cost of losing a proportion of tall trees (e.g., up to ~30%).

5. Conclusion

California’s dry forest ecosystems, and others across western North America, face a potentially grave future under climate change (AghaKouchak et al., 2014; Westerling, 2016; Liang et al., 2017; Schoennagel et al., 2017). With a strong legacy of fire suppression, fuel accumulation, and loss of keystone old trees (Knapp et al., 2013; Hagemann et al., 2021), coupled with an increasingly warmer and drier climate and extended fire seasons (Westerling, 2016; Pierce et al., 2018; Williams et al., 2019), there is no wonder why the majority of recent research on dry forest resistance and resilience portray a mostly dire situation (Coop et al., 2020). Indeed, the 2012–2016 drought resulted in significant mortality across the Sierra Nevada (especially the southern half of the range) with a particularly strong impact on perhaps the most critical and fire-resistant trees (Fettig et al., 2019). Moreover, other studies document rapid increases in fire size, severity, and high-severity patch sizes in California over recent decades (Stevens et al., 2017; Steel et al., 2018; Cova et al., 2023), projecting similarly negative trends for future decades (Abatzoglou and Williams, 2016; Williams et al., 2019). Undoubtedly, recent impacts from fire and drought are unprecedented and have serious implications for the sustainability of dry forest ecosystems and the suite of valued resources they provide (Coop et al., 2020; Steel et al., 2023).

Our study provides a degree of contrast against this largely negative environmental narrative. We demonstrate what could be achieved if intentional, ecologically-centered policies and management practices are adopted (Hessburg et al., 2021; Meyer et al., 2021; Prichard et al., 2021). For example, several recent studies have proposed landscape-level forest management strategies which delineate large landscapes, generally far from the wildland urban interface, where more proactive fire management strategies can be practiced to support the reintroduction of low- to moderate-severity fires (North et al., 2021, 2024). North et al. (2024) show that large portions of existing dry forest landscapes across western North America are well positioned for this type of management and could be used to increase the total extent of active-fire landscapes. Our study suggests that proactive management strategies like these, focused on restoring the key process of fire to fire-adapted forests, can help bolster forest resistance and contribute to

the long-term sustainability of dry forest ecosystems.

Data statement

Data will be made available on request.

CRedit authorship contribution statement

Caden P. Chamberlain: Writing – original draft, Visualization, Software, Methodology, Funding acquisition, Formal analysis, Data curation, Conceptualization. **Liz van Wagendonk:** Writing – review & editing, Methodology, Conceptualization. **Bryce Bartl-Geller:** Writing – review & editing, Methodology, Conceptualization. **Malcolm P. North:** Writing – review & editing, Methodology, Conceptualization. **C. Alina Cansler:** Writing – review & editing, Supervision, Methodology, Funding acquisition, Conceptualization. **Marc D. Meyer:** Writing – review & editing, Methodology, Conceptualization. **Chad T. Anderson:** Writing – review & editing, Methodology, Data curation. **Van R. Kane:** Writing – review & editing, Supervision, Methodology, Funding acquisition, Conceptualization.

Funding

This work was supported by the National Aeronautics and Space Administration (grant number 80NSSC21K1588), the Joint Fire Science Program (grant number 23-1-01-11), and the CAL FIRE Forest Health Research Program (grant number (8GG22810).

Declaration of Competing Interest

The authors declare that they have no known competing financial interests or personal relationships that could have appeared to influence the work reported in this paper.

Acknowledgements

We thank L. Monika Moskal and Brian Harvey for their friendly reviews of the initial versions of this manuscript and the general study design.

Appendix A. Supporting information

Supplementary data associated with this article can be found in the online version at [doi:10.1016/j.foreco.2025.123345](https://doi.org/10.1016/j.foreco.2025.123345).

Data availability

There is a link to the data and code on the main text cover page.

References

Abatzoglou, J.T., 2013. Development of gridded surface meteorological data for ecological applications and modelling. *Int. J. Climatol.* 33, 121–131. <https://doi.org/10.1002/joc.3413>.

Abatzoglou, J.T., Williams, A.P., 2016. Impact of anthropogenic climate change on wildfire across western US forests. *Proc. Natl. Acad. Sci.* 113 (42), 11770–11775. <https://doi.org/10.1073/pnas.1607171113>.

Abella, S.R., Denton, C.W., 2009. Spatial variation in reference conditions: historical tree density and pattern on a *Pinus ponderosa* landscape. *Can. J. For. Res.* 39 (12), 2391–2403. <https://doi.org/10.1139/X09-146>.

AghaKouchak, A., Cheng, L., Mazdiyasni, O., Farahmand, A., 2014. Global warming and changes in risk of concurrent climate extremes: insights from the 2014 California drought. *Geophys. Res. Lett.* 41 (24), 8847–8852. <https://doi.org/10.1002/2014GL062308>.

Atchley, A.L., Linn, R., Jonko, A., Hoffman, C., Hyman, J.D., Pimont, F., Sieg, C., Middleton, R.S., Atchley, A.L., Linn, R., et al., 2021. Effects of fuel spatial distribution on wildland fire behaviour. *Int. J. Wildland Fire* 30 (3), 179–189. <https://doi.org/10.1071/WF20096>.

Bjornstad O.N. 2022. ncf: Spatial Covariance Functions. R package version 1.3-2. (<http://CRAN.R-project.org/package=ncf>).

Blackburn, R.C., Buscaglia, R., Sánchez Meador, A.J., Moore, M.M., Sankey, T., Sesnie, S.E., 2025. Eigenfeature-enhanced deep learning: advancing tree species classification in mixed conifer forests with lidar. *Remote Sens. Ecol. Conserv.* <https://doi.org/10.1002/rse2.70014>.

Blomdahl, E.M., Thompson, C.M., Kane, J.R., Kane, V.R., Churchill, D., Moskal, L.M., Lutz, J.A., 2019. Forest structure predictive of fisher (*Pekania pennanti*) dens exists in recently burned forest in Yosemite, California, USA. *For. Ecol. Manag.* 444, 174–186. <https://doi.org/10.1016/j.foreco.2019.04.024>.

Boisramé, G., Thompson, S., Collins, B., Stephens, S., 2017. Managed wildfire effects on forest resilience and water in the Sierra Nevada. *Ecosystems* 20 (4), 717–732. <https://doi.org/10.1007/s10021-016-0048-1>.

Buma, B., 2015. Disturbance interactions: characterization, prediction, and the potential for cascading effects. *art70 Ecosphere* 6 (4). <https://doi.org/10.1890/ES15-00058.1>.

Cansler, C.A., Hood, S.M., van Mantgem, P.J., Varner, J.M., 2020. A large database supports the use of simple models of post-fire tree mortality for thick-barked conifers, with less support for other species. *Fire Ecol.* 16, 25. <https://doi.org/10.1186/s42408-020-00082-0>.

Cansler, C.A., Swanson, M.E., Furniss, T.J., Larson, A.J., Lutz, J.A., 2019. Fuel dynamics after reintroduced fire in an old-growth Sierra Nevada mixed-conifer forest. *Fire Ecol.* 15 (1), 16. <https://doi.org/10.1186/s42408-019-0035-y>.

Chamberlain, C.P., Bartl-Geller, B.N., Cansler, C.A., North, M.P., Meyer, M.D., van Wagendonk, L., Redford, H.E., Kane, V.R., 2024. When do contemporary wildfires restore forest structures in the Sierra Nevada? *Fire Ecol.* 20 (1), 91. <https://doi.org/10.1186/s42408-024-00324-5>.

Chamberlain, C.P., Cova, G.R., Cansler, C.A., North, M.P., Meyer, M.D., Jeronimo, S.M.A., Kane, V.R., 2023a. Consistently heterogeneous structures observed at multiple spatial scales across fire-intact reference sites. *For. Ecol. Manag.* 550, 121478. <https://doi.org/10.1016/j.foreco.2023.121478>.

Chamberlain, C.P., Cova, G.R., Kane, V.R., Cansler, C.A., Kane, J.T., Bartl-Geller, B.N., van Wagendonk, L., Jeronimo, S.M., Stine, P., North, M.P., 2023b. Sierra Nevada reference conditions: A dataset of contemporary reference sites and corresponding remote sensing-derived forest structure metrics for yellow pine and mixed-conifer forests. *Data Brief.* 51, 109807.

Churchill, D.J., Larson, A.J., Dahlgreen, M.C., Franklin, J.F., Hessburg, P.F., Lutz, J.A., 2013. Restoring forest resilience: from reference spatial patterns to silvicultural prescriptions and monitoring. *For. Ecol. Manag.* 291, 442–457. <https://doi.org/10.1016/j.foreco.2012.11.007>.

Collins, B.M., Everett, R.G., Stephens, S.L., 2011a. Impacts of fire exclusion and recent managed fire on forest structure in old growth Sierra Nevada mixed-conifer forests. *Ecosphere* 2 (4), art51. <https://doi.org/10.1890/ES11-00026.1>.

Collins, B.M., Kelly, M., van Wagendonk, J.W., Stephens, S.L., 2007. Spatial patterns of large natural fires in Sierra Nevada wilderness areas. *Landsc. Ecol.* 22 (4), 545–557. <https://doi.org/10.1007/s10980-006-9047-5>.

Collins, B.M., Lydersen, J.M., Everett, R.G., Fry, D.L., Stephens, S.L., 2015. Novel characterization of landscape-level variability in historical vegetation structure. *Ecol. Appl.* 25 (5), 1167–1174. <https://doi.org/10.1890/14-1797.1>.

Collins, B.M., Lydersen, J.M., Everett, R.G., Stephens, S.L., 2018. How does forest recovery following moderate-severity fire influence effects of subsequent wildfire in mixed-conifer forests? *Fire Ecol.* 14 (2), 3. <https://doi.org/10.1186/s42408-018-0004-x>.

Collins, B.M., Lydersen, J.M., Fry, D.L., Wilkin, K., Moody, T., Stephens, S.L., 2016. Variability in vegetation and surface fuels across mixed-conifer-dominated landscapes with over 40 years of natural fire. *For. Ecol. Manag.* 381, 74–83. <https://doi.org/10.1016/j.foreco.2016.09.010>.

Collins, B.M., Stephens, S.L., 2007. Managing natural wildfires in Sierra Nevada wilderness areas. *Front. Ecol. Environ.* 5, 523–527. <https://doi.org/10.1890/070007>.

Coop, J.D., Parks, S.A., Stevens-Rumann, C.S., Crausbay, S.D., Higuera, P.E., Hurteau, M.D., Tepley, A., Whitman, E., Assal, T., Collins, B.M., et al., 2020. Wildfire-driven forest conversion in western North American landscapes. *BioScience* 70 (8), 659–673. <https://doi.org/10.1093/biosci/biaa061>.

Cova, G., Kane, V.R., Prichard, S., North, M., Cansler, C.A., 2023. The outsized role of California's largest wildfires in changing forest burn patterns and coarsening ecosystem scale. *For. Ecol. Manag.* 528, 120620. <https://doi.org/10.1016/j.foreco.2022.120620>.

Das, A.J., Slaton, M.R., Mallory, J., Asner, G.P., Martin, R.E., Hardwick, P., 2022. Empirically validated drought vulnerability mapping in the mixed conifer forests of the Sierra Nevada. *Ecol. Appl.* 32 (2), e2514. <https://doi.org/10.1002/earp.2514>.

Das, A.J., Stephenson, N.L., Davis, K.P., 2016. Why do trees die? Characterizing the drivers of background tree mortality. *Ecology* 97 (10), 2616–2627. <https://doi.org/10.1002/ecy.1497>.

Davis, K.T., Peeler, J., Fargione, J., Haugo, R.D., Metlen, K.L., Robles, M.D., Woolley, T., 2024. Tamm review: A meta-analysis of thinning, prescribed fire, and wildfire effects on subsequent wildfire severity in conifer dominated forests of the Western US. *For. Ecol. Manag.* 561, 121885. <https://doi.org/10.1016/j.foreco.2024.121885>.

Falk, D.A., Heyerdahl, E.K., Brown, P.M., Farris, C., Fulé, P.Z., McKenzie, D., Swetnam, T.W., Taylor, A.H., van Horne, M.L., 2011. Multi-scale controls of historical forest-fire regimes: new insights from fire-scar networks. *Front. Ecol. Environ.* 9 (8), 446–454. [https://doi.org/10.1080/100052](https://doi.org/10.1080/10.1080/100052).

Falk, D.A., van Mantgem, P.J., Keeley, J.E., Gregg, R.M., Guiterman, C.H., Tepley, A.J., JN Young, D., Marshall, L.A., 2022. Mechanisms of forest resilience. *For. Ecol. Manag.* 512, 120129. <https://doi.org/10.1016/j.foreco.2022.120129>.

Faraway J.J. 2015. Linear Models with R, 2nd ed. Chapman and Hall/CRC Texts in Statistical Science, New York.

Fettig, C.J., Klepzig, K.D., Billings, R.F., Munson, A.S., Nebeker, T.E., Negrón, J.F., Nowak, J.T., 2007. The effectiveness of vegetation management practices for prevention and control of bark beetle infestations in coniferous forests of the western

and southern United States. *For. Ecol. Manag.* 238 (1), 24–53. <https://doi.org/10.1016/j.foreco.2006.10.011>.

Fettig, C.J., Mortenson, L.A., Bulaon, B.M., Foulk, P.B., 2019. Tree mortality following drought in the central and southern Sierra Nevada, California, U.S. *For. Ecol. Manag.* 432, 164–178. <https://doi.org/10.1016/j.foreco.2018.09.006>.

Flint, L.E., Flint, A.L., Stern, M.A., 2021. The basin characterization model—A regional water balance software package. Reston, VA: U.S. Geological Survey Techniques and Methods Report No.: 6-H1. [Accessed 2022 Dec 8]. (<http://pubs.er.usgs.gov/publication/tm6H1>).

FRAP. 2021. California Department of Forestry and Fire Protection's Fire and Resource Assessment Program. [accessed July 2021]. (<https://frap.fire.ca.gov/mapping/gis-data/>).

Furniss, T.J., Das, A.J., van Mantgem, P.J., Stephenson, N.L., Lutz, J.A., 2022. Crowding, climate, and the case for social distancing among trees. *Ecol. Appl.* 32 (2), e2507. <https://doi.org/10.1002/eaap.2507>.

Furniss, T.J., Larson, A.J., Kane, V.R., Lutz, J.A., 2020. Wildfire and drought moderate the spatial elements of tree mortality. *Ecosphere* 11 (8), e03214. <https://doi.org/10.1002/ecs2.3214>.

Germain, S.J., Lutz, J.A., 2024. Stand diversity increases pine resistance and resilience to compound disturbance. *Fire Ecol.* 20 (1), 53. <https://doi.org/10.1186/s42408-024-00283-x>.

Griffin, D., Anchukaitis, K.J., 2014. How unusual is the 2012–2014 California drought? *Geophys. Res. Lett.* 41 (24), 9017–9023. <https://doi.org/10.1002/2014GL062433>.

Hagmann, R.K., Hessburg, P.F., Prichard, S.J., Povak, N.A., Brown, P.M., Fulé, P.Z., Keane, R.E., Knapp, E.E., Lydersen, J.M., Metlen, K.L., et al., 2021. Evidence for widespread changes in the structure, composition, and fire regimes of western North American forests. *Ecol. Appl.* 31 (8), 24–31. <https://doi.org/10.1002/eaap.2431>.

Hankin, L.E., Anderson, C.T., 2022. Second-entry burns reduce mid-canopy fuels and create resilient forest structure in Yosemite National Park, California. *Forests* 13 (9), 1512. <https://doi.org/10.3390/f13091512>.

Hankin, L.E., Crumrine, S.A., Anderson, C.T., 2024. Impacts of mega drought in fire-prone montane forests and implications for forest management. *For. Ecol. Manag.* 564, 122010. <https://doi.org/10.1016/j.foreco.2024.122010>.

Hessburg, P.F., Churchill, D.J., Larson, A.J., Haugo, R.D., Miller, C., Spies, T.A., North, M.P., Povak, N.A., Belote, R.T., Singleton, P.H., et al., 2015. Restoring fire-prone Inland Pacific landscapes: seven core principles. *Landscape Ecol.* 30 (10), 1805–1835. <https://doi.org/10.1007/s10980-015-0218-0>.

Hessburg, P.F., Miller, C.L., Parks, S.A., Povak, N.A., Taylor, A.H., Higuera, P.E., Prichard, S.J., North, M.P., Collins, B.M., Hurteau, M.D., et al., 2019. Climate, environment, and disturbance history Govern resilience of western North American forests. *Front. Ecol. Evol.* 7. <https://doi.org/10.3389/fevo.2019.00239>.

Hessburg, P.F., Prichard, S.J., Hagmann, R.K., Povak, N.A., Lake, F.K., 2021. Wildfire and climate change adaptation of western North American forests: a case for intentional management. *Ecol. Appl.* 31 (8), e02432. <https://doi.org/10.1002/eaap.2432>.

Hood, S., Sala, A., Heyerdahl, E.K., Boutin, M., 2015. Low-severity fire increases tree defense against bark beetle attacks. *Ecology* 96 (7), 1846–1855. <https://doi.org/10.1890/14-0487.1>.

Hood, S.M., Varner, J.M., Jain, T.B., Kane, J.M., 2022. A framework for quantifying forest wildfire hazard and fuel treatment effectiveness from stands to landscapes. *Fire Ecol.* 18 (1), 33. <https://doi.org/10.1186/s42408-022-00157-0>.

Housman, I., Campbell, L., Heyer, J., Goetz, W., Finco, M., Pugh, N., 2022. US Forest Service Landscape Change Monitoring System Methods. Version 2021.7.

Huffman, D.W., Roccaforte, J.P., Springer, J.D., Crouse, J.E., 2020. Restoration applications of resource objective wildfires in western US forests: a status of knowledge review. *Fire Ecol.* 16 (1), 18. <https://doi.org/10.1186/s42408-020-00077-x>.

Hurteau, M.D., Goodwin, M.J., Marsh, C., Zald, H.S., Collins, B., Meyer, M., North, M.P., 2024. Managing fire-prone forests in a time of decreasing carbon carrying capacity. *Front. Ecol. Environ.* 22 (10), e2801. <https://doi.org/10.1002/fee.2801>.

Jenness, J., 2007. Some Thoughts on Analyzing Topographic Habitat Characteristics. Jenness Enterprises, Flagstaff, AZ, USA, p. 26.

Jeronimo, S.M.A., Kane, V.R., Churchill, D.J., McGaughey, R.J., Franklin, J.F., 2018. Applying LiDAR individual tree detection to management of structurally diverse forest landscapes. *J. For.* 116 (4), 336–346. <https://doi.org/10.1093/jofore/fvy023>.

Jeronimo, S.M.A., Kane, V.R., Churchill, D.J., Lutz, J.A., North, M.P., Asner, G.P., Franklin, J.F., 2019. Forest structure and pattern vary by climate and landform across active-fire landscapes in the montane Sierra Nevada. *For. Ecol. Manag.* 437, 70–86. <https://doi.org/10.1016/j.foreco.2019.01.033>.

Johnstone, J.F., Allen, C.D., Franklin, J.F., Frelich, L.E., Harvey, B.J., Higuera, P.E., Mack, M.C., Meentemeyer, R.K., Metz, M.R., Perry, G.L., et al., 2016. Changing disturbance regimes, ecological memory, and forest resilience. *Front. Ecol. Environ.* 14 (7), 369–378. <https://doi.org/10.1002/fee.1311>.

Kaartinen, H., Hyypä, J., Yu, X., Vastaranta, M., Hyypä, H., Kukko, A., Holopainen, M., Heipke, C., Hirschmugl, M., Morsdorf, F., et al., 2012. An international comparison of individual tree detection and extraction using airborne laser scanning. *Remote Sens.* 4 (4), 950–974. <https://doi.org/10.3390/rs4040950>.

Kane, V.R., Bartl-Geller, B.N., Cova, G.R., Chamberlain, C.P., van Wagendonk, L., North, M.P., 2023. Where are the large trees? A census of Sierra Nevada large trees to determine their frequency and spatial distribution across three large landscapes. *For. Ecol. Manag.* 546, 121351. <https://doi.org/10.1016/j.foreco.2023.121351>.

Kane, V.R., Bartl-Geller, B.N., North, M.P., Kane, J.T., Lydersen, J.M., Jeronimo, S.M.A., Collins, B.M., Monika Moskal, L., 2019. First-entry wildfires can create opening and tree clump patterns characteristic of resilient forests. *For. Ecol. Manag.* 454, 117659. <https://doi.org/10.1016/j.foreco.2019.117659>.

Kane, V.R., Cansler, C.A., Povak, N.A., et al., 2015a. Mixed severity fire effects within the Rim fire: Relative importance of local climate, fire weather, topography, and forest structure. *For. Ecol. Manag.* 358, 62–79. <https://doi.org/10.1016/j.foreco.2015.09.001>.

Kane, V.R., Lutz, J.A., Cansler, C.A., Povak, N.A., Churchill, D.J., Smith, D.F., Kane, J.T., North, M.P., 2015b. Water balance and topography predict fire and forest structure patterns. *For. Ecol. Manag.* 338, 1–13. <https://doi.org/10.1016/j.foreco.2014.10.038>.

Kane, V.R., Lutz, J.A., Roberts, S.L., Smith, D.F., McGaughey, R.J., Povak, N.A., Brooks, M.L., 2013. Landscape-scale effects of fire severity on mixed-conifer and red fir forest structure in Yosemite National Park. *For. Ecol. Manag.* 287, 17–31. <https://doi.org/10.1016/j.foreco.2012.08.044>.

Kane, V.R., North, M.P., Lutz, J.A., Churchill, D.J., Roberts, S.L., Smith, D.F., McGaughey, R.J., Kane, J.T., Brooks, M.L., 2014. Assessing fire effects on forest spatial structure using a fusion of Landsat and airborne LiDAR data in Yosemite National Park. *Remote Sens. Environ.* 151, 89–101. <https://doi.org/10.1016/j.rse.2013.07.041>.

Kane, J.M., Varner, J.M., Metz, M.R., van Mantgem, P.J., 2017. Characterizing interactions between fire and other disturbances and their impacts on tree mortality in western U.S. Forests. *For. Ecol. Manag.* 405, 188–199. <https://doi.org/10.1016/j.foreco.2017.09.037>.

Keeley, J.E., 2012. Ecology and evolution of pine life histories. *Ann. For. Sci.* 69 (4), 445–453. <https://doi.org/10.1007/s13595-012-0201-8>.

Key, C.H., Benson, N.C., 2006. Landscape Assessment (LA). FIREMON: Fire Effects Monitoring and Inventory System 164: LA – 1. (https://gsp.humboldt.edu/OLM/Courses/GSP_216).

Khatri-Chhetri, P., van Wagendonk, L., Hendryx, S.M., Kane, V.R., 2024. Enhancing individual tree mortality mapping: the impact of models, data modalities, and classification taxonomy. *Remote Sens. Environ.* 300, 113914. <https://doi.org/10.1016/j.rse.2023.113914>.

Klimaszewski-Patterson, A., Dingemans, T., Morgan, C.T., Mensing, S.A., 2024. Human influence on late Holocene fire history in a mixed-conifer forest, Sierra National Forest, California. *Fire Ecol.* 20, 3. <https://doi.org/10.1186/s42408-023-00245-9>.

Knapp, E.E., Bernal, A.A., Kane, J.M., Fettig, C.J., North, M.P., 2021. Variable thinning and prescribed fire influence tree mortality and growth during and after a severe drought. *For. Ecol. Manag.* 479, 118595. <https://doi.org/10.1016/j.foreco.2020.118595>.

Knapp, E.E., Skinner, C.N., North, M.P., Estes, B.L., 2013. Long-term overstory and understory change following logging and fire exclusion in a Sierra Nevada mixed-conifer forest. *For. Ecol. Manag.* 310, 903–914. <https://doi.org/10.1016/j.foreco.2013.09.041>.

Koontz, M.J., Latimer, A.M., Mortenson, L.A., Fettig, C.J., North, M.P., 2021. Cross-scale interaction of host tree size and climatic water deficit governs bark beetle-induced tree mortality. *Nat. Commun.* 12 (1), 129. <https://doi.org/10.1038/s41467-020-20455-y>.

Koontz, M.J., North, M.P., Werner, C.M., Fick, S.E., Latimer, A.M., 2020. Local forest structure variability increases resilience to wildfire in dry western U.S. coniferous forests. *Ecol. Lett.* 23 (3), 483–494. <https://doi.org/10.1111/ele.13447>.

Kramer, H.A., Jones, G.M., Kane, V.R., Bartl-Geller, B., Kane, J.T., Whitmore, S.A., Berigan, W.J., Dotters, B.P., Roberts, K.N., Sawyer, S.C., Keane, J.J., North, M.P., Gutierrez, R.J., Peery, M.Z., 2021. Elevational gradients strongly mediate habitat selection patterns in a nocturnal predator. *Ecosphere* 12, e03500. <https://doi.org/10.1002/ecs.23500>.

Kreider, M.R., Higuera, P.E., Parks, S.A., Rice, W.L., White, N., Larson, A.J., 2024. Fire suppression makes wildfires more severe and accentuates impacts of climate change and fuel accumulation. *Nat. Commun.* 15 (1), 2412. <https://doi.org/10.1038/s41467-024-46702-0>.

Kuhn, M., Wickham, H., 2020. tidymodels a Collect. Packages Model. Mach. Learn. Using tidyverse Princ. (<https://www.tidymodels.org>).

Larson, A.J., Belote, R.T., Cansler, C.A., Parks, S.A., Dietz, M.S., 2013. Latent resilience in ponderosa pine forest: effects of resumed frequent fire. *Ecol. Appl.* 23 (6), 1243–1249. <https://doi.org/10.1890/13-0066.1>.

Larson, A.J., Churchill, D., 2012. Tree spatial patterns in fire-frequent forests of western North America, including mechanisms of pattern formation and implications for designing fuel reduction and restoration treatments. *For. Ecol. Manag.* 267, 74–92. <https://doi.org/10.1016/j.foreco.2011.11.038>.

Larson, A.J., Jeronimo, S.M.A., Hessburg, P.F., Lutz, J.A., Povak, N.A., Cansler, C.A., Kane, V.R., Churchill, D.J., 2022. Tamm review: ecological principles to guide post-fire forest landscape management in the Inland Pacific and Northern Rocky Mountain regions. *For. Ecol. Manag.* 504, 119680. <https://doi.org/10.1016/j.foreco.2021.119680>.

Liang, S., Hurteau, M.D., Westerling, A.L., 2017. Response of Sierra Nevada forests to projected climate-wildfire interactions. *Glob. Change Biol.* 23 (5), 2016–2030. <https://doi.org/10.1111/gcb.13544>.

Lloret, F., Escudero, A., Iriondo, J.M., Martínez-Vilalta, J., Valladares, F., 2012. Extreme climatic events and vegetation: the role of stabilizing processes. *Glob. Change Biol.* 18 (3), 797–805. <https://doi.org/10.1111/j.1365-2486.2011.02624.x>.

Lutz, J.A., Larson, A.J., Swanson, M.E., Freund, J.A., 2012. Ecological importance of large-diameter trees in a temperate mixed-conifer forest. *PLOS ONE* 7 (5), e36131. <https://doi.org/10.1371/journal.pone.0036131>.

Lydersen, J.M., North, M.P., 2012. Topographic variation in active-fire forest structure under current climate conditions. *Ecosystems* 15, 1134–1146. <https://doi.org/10.1007/s10021-012-9573-8>.

Lydersen, J.M., North, M.P., Collins, B.M., 2014. Severity of an uncharacteristically large wildfire, the Rim Fire, in forests with relatively restored frequent fire regimes. *For. Ecol. Manag.* 328, 326–334. <https://doi.org/10.1016/j.foreco.2014.06.005>.

Lydersen, J.M., North, M.P., Knapp, E.E., Collins, B.M., 2013. Quantifying spatial patterns of tree groups and gaps in mixed-conifer forests: reference conditions and

long-term changes following fire suppression and logging. *For. Ecol. Manag.* 304, 370–382. <https://doi.org/10.1016/j.foreco.2013.05.023>.

Marlon, J.R., Bartlein, P.J., Gavin, D.G., Long, C.J., Anderson, R.S., Briles, C.E., Brown, K.J., Colombaroli, D., Hallett, D.J., Power, M.J., et al., 2012. Long-term perspective on wildfires in the western USA. *Proc. Natl. Acad. Sci.* 109 (9). <https://doi.org/10.1073/pnas.1112839109>.

Marra, G., Wood, S.N., 2011. Practical variable selection for generalized additive models. *Comput. Stat. Data Anal.* 55 (7), 2372–2387. <https://doi.org/10.1016/j.csda.2011.02.004>.

Marvin, N.W., Ziegler, A., 2017. Ranger: a fast implementation of random forests for high dimensional data in C++ and R. *J. Stat. Softw.* 77, 1–17. <https://doi.org/10.18637/jss.v077.i01>.

Mast, J.N., Veblen, T.T., 1999. Tree spatial patterns and stand development along the pine-grassland ecotone in the Colorado Front Range. *Can. J. For. Res.* 29 (5), 575–584. <https://doi.org/10.1139/x99-025>.

May, C.J., Zald, H.S.J., North, M.P., Gray, A.N., Hurteau, M.D., 2023. Repeated burns fail to restore pine regeneration to the natural range of variability in a Sierra Nevada mixed-conifer forest, U.S.A. *Restor. Ecol.* 31 (5), e13863. <https://doi.org/10.1111/rec.13863>.

McGaughey, R.J., 2020. FUSION/LDV: Software for LIDAR Data Analysis and Visualization: Version 4.00. USDA Forest Service Pacific Northwest Research Station, Seattle, WA. (http://forsys.cfr.washington.edu/FUSION/fusion_overview.html).

McLachlan, K.K., Higuera, P.E., Miesel, J., Rogers, B.M., Schweitzer, J., Shuman, J.K., Tepley, A.J., Varner, J.M., Veblen, T.T., Adalsteinsson, S.A., et al., 2020. Fire as a fundamental ecological process: research advances and frontiers. *J. Ecol.* 108 (5), 2047–2069. <https://doi.org/10.1111/1365-2745.13403>.

Meyer, M.D., Long, J.W., Safford, H.D., 2021. Postfire Restoration Framework for National forests in California. US Department of Agriculture, Forest Service, Pacific Southwest Research Station. PSW-GTR-270. 1–204. (<https://www.fs.usda.gov/research/treeseach/61909>).

Mitchell, B., Fisk, H., Clark, J., et al., 2018. Lidar Acquisition Specifications for Forestry Applications. US Forest Service, Geospatial Technology & Applications Centre, Salt Lake City, UT, USA.

Murphy, J.S., York, R., Rivera Huerta, H., Stephens, S.L., 2021. Characteristics and metrics of resilient forests in the Sierra de San Pedro Martir, Mexico. *For. Ecol. Manag.* 482, 118864. <https://doi.org/10.1016/j.foreco.2020.118864>.

Ng, J., North, M.P., Arditti, A.J., Cooper, M.R., Lutz, J.A., 2020. Topographic variation in tree group and gap structure in Sierra Nevada mixed-conifer forests with active fire regimes. *For. Ecol. Manag.* 472, 118220. <https://doi.org/10.1016/j.foreco.2020.118220>.

North, M.P., Bisbing, S.M., Hankins, D.L., Hessburg, P.F., Hurteau, M.D., Kobziar, L.N., Meyer, M.D., Rhea, A.E., Stephens, S.L., Stevens-Rumann, C.S., 2024. Strategic fire zones are essential to wildfire risk reduction in the Western United States. *Fire Ecol.* 20 (1), 50. <https://doi.org/10.1186/s42408-024-00282-y>.

North, M.P., Kane, J.T., Kane, V.R., Asner, P., Berigan, W., Churchill, D.J., Conway, S., Gutiérrez, R.J., Jeronimo, S.M.A., Keane, J., Koltunov, A., Mark, T., Moskal, L.M., Munton, T., Peery, Z., Ramirez, C., Sollmann, R., White, A.M., Whitmore, S., 2017. Cover of tall trees best predicts California spotted owl habitat. *For. Ecol. Manag.* 405, 166–178. <https://doi.org/10.1016/j.foreco.2017.09.019>.

North, M.P., Stine, P., O'Hara K., Zielinski W., Stephens S. 2009. An ecosystem management strategy for Sierran mixed-conifer forests. US Department of Agriculture, Forest Service, Pacific Southwest Research Station. PSW-GTR-2020. (<http://www.fs.usda.gov/treeseach/pubs/32916>).

North, M.P., York, R.A., Collins, B.M., Hurteau, M.D., Jones, G.M., Knapp, E.E., Kobziar, L., McCann, H., Meyer, M.D., Stephens, S.L., et al., 2021. Pyrosilviculture needed for landscape resilience of dry western United States forests. *J. For.* 119 (5), 520–544. <https://doi.org/10.1093/jofore/fvab026>.

Parks, S.A., 2014. Mapping day-of-burning with coarse-resolution satellite fire-detection data. *Int. J. Wildland Fire* 23, 215–223. <https://doi.org/10.1071/WF13138>.

Parks, S.A., Holsinger, L.M., Koontz, M.J., Collins, L., Whitman, E., Parisien, M.A., Loehman, R.A., Barnes, J.L., Bourdon, J.F., Boucher, J., et al., 2019. Giving ecological meaning to satellite-derived fire severity metrics across North American forests. *Remote Sens.* 11 (14), 14. <https://doi.org/10.3390/rs11141735>.

Pawlowski, N.C., Coppoletta, M., Knapp, E., Taylor, A.H., 2019. Spatial dynamics of tree group and gap structure in an old-growth ponderosa pine-California black oak forest burned by repeated wildfires. *For. Ecol. Manag.* 434, 289–302. <https://doi.org/10.1016/j.foreco.2018.12.016>.

Pierce, D.W., Kalansky, J.F., Cayan, D.R., 2018. Calif. 'S. Fourth Clim. Change Assess. (<https://www.climateassessment.ca.gov/>).

Ploton, P., Mortier, F., Réjou-Méchain, M., Barbier, N., Picard, N., Rossi, V., Dormann, C., Cornu, G., Viennois, G., Bayol, N., Lyapustin, A., 2020. Spatial validation reveals poor predictive performance of large-scale ecological mapping models. *Nat. Commun.* 11 (1), 4540. <https://doi.org/10.1038/s41467-020-18321-y>.

Prichard, S.J., Hessburg, P.F., Hagmann, R.K., Povak, N.A., Dobrowski, S.Z., Hurteau, M.D., Kane, V.R., Keane, R.E., Kobziar, L.N., Kolden, C.A., et al., 2021. Adapting western North American forests to climate change and wildfires: 10 common questions. *Ecol. Appl.* 31 (8), e02433. <https://doi.org/10.1002/eaap.2433>.

R Core Team, 2024. R version 4.3.3: R: a language and environment for statistical computing. R Foundation for Statistical Computing, Vienna, Austria.

Reed, C.C., Hood, S.M., Cluck, D.R., Smith, S.L., 2023. Fuels change quickly after California drought and bark beetle outbreaks with implications for potential fire behavior and emissions. *Fire Ecol.* 19, 16. <https://doi.org/10.1186/s42408-023-00175-6>.

Restaino, C., Young, D.J.N., Estes, B., Gross, S., Wuenschel, A., Meyer, M., Safford, H., 2019. Forest structure and climate mediate drought-induced tree mortality in forests of the Sierra Nevada, USA. *Ecol. Appl.* 29 (4), e01902. <https://doi.org/10.1002/eaap.1902>.

Ritter, S.M., Hoffman, C.M., Battaglia, M.A., Stevens-Rumann, C.S., Mell, W.E., 2020. Fine-scale fire patterns mediate forest structure in frequent-fire ecosystems. *Ecosphere* 11 (7), e03177. <https://doi.org/10.1002/ecs2.3177>.

Roberts, D.W., Cooper, S.V., 1989. Concepts and techniques of vegetation mapping. In: *Land Classifications Based on Vegetation: Applications for Resource Management*. US Department of Agriculture, Forest Service, GTR INT-257. 90–96.

Safford, H.D., Stevens, J.T., 2017. Natural range of variation for yellow pine and mixed-conifer forests in the Sierra Nevada, southern Cascades, and Modoc and Inyo National Forests, California, USA. Forests. US Department of Agriculture, Forest Service, Pacific Southwest Research Station. Gen. Tech. Rep. PSW-GTR-256. (<http://www.fs.usda.gov/treeseach/pubs/55393>).

Schoennagel, T., Balch, J.K., Brenkert-Smith, H., Dennison, P.E., Harvey, B.J., Krawchuk, M.A., Mietkiewicz, N., Morgan, P., Moritz, M.A., Rasker, R., et al., 2017. Adapt to more wildfire in western North American forests as climate changes. *Proc. Natl. Acad. Sci.* 114 (18), 4582–4590. <https://doi.org/10.1073/pnas.1617464114>.

Sparks, A.M., Corrao, M.V., Smith, A.M.S., 2022. Cross-comparison of individual tree detection methods using low and high pulse density airborne laser scanning data. *Remote Sens.* 14 (14), 3480. <https://doi.org/10.3390/rs14143480>.

Steel, Z.L., Foster, D., Coppoletta, M., Lydersen, J.M., Stephens, S.L., Paudel, A., Markwith, S.H., Merriam, K., Collins, B.M., 2021a. Ecological resilience and vegetation transition in the face of two successive large wildfires. *J. Ecol.* 109 (9), 3340–3355. <https://doi.org/10.1111/1365-2745.13764>.

Steel, Z.L., Goodwin, M.J., Meyer, M.D., Fricker, G.A., Zald, H.S.J., Hurteau, M.D., North, M.P., 2021b. Do forest fuel reduction treatments confer resistance to beetle infestation and drought mortality? *Ecosphere* 12 (1), e03344. <https://doi.org/10.1002/ecs2.3344>.

Steel, Z.L., Jones, G.M., Collins, B.M., Green, R., Koltunov, A., Purcell, K.L., Sawyer, S.C., Slatton, M.R., Stephens, S.L., Stine, P., et al., 2023. Mega-disturbances cause rapid decline of mature conifer forest habitat in California. *Ecol. Appl.* 33 (2), e2763. <https://doi.org/10.1002/eaap.2763>.

Steel, Z.L., Koontz, M.J., Safford, H.D., 2018. The changing landscape of wildfire: burn pattern trends and implications for California's yellow pine and mixed conifer forests. *Landsc. Ecol.* 33 (7), 1159–1176. <https://doi.org/10.1007/s10980-018-0665-5>.

Stephens, S.L., Collins, B.M., Biber, E., Fulé, P.Z., 2016a. U.S. federal fire and forest policy: emphasizing resilience in dry forests. *Ecosphere* 7 (11), e01584. <https://doi.org/10.1002/ecs2.1584>.

Stephens, S.L., Fry, D.L., Franco-Vizcaíno, E., 2008. Wildfire and spatial patterns in forests in northwestern Mexico: the United States wishes it had similar fire problems. *Ecol. Soc.* 13 (2). (<https://www.jstor.org/stable/26267961>).

Stephenson, N., 1998. Actual evapotranspiration and deficit: biologically meaningful correlates of vegetation distribution across spatial scales. *J. Biogeogr.* 25 (5), 855–870. <https://doi.org/10.1046/j.1365-2699.1998.00233.x>.

Stevens, J.T., Collins, B.M., Miller, J.D., North, M.P., Stephens, S.L., 2017. Changing spatial patterns of stand-replacing fire in California conifer forests. *For. Ecol. Manag.* 406, 28–36. <https://doi.org/10.1016/j.foreco.2017.08.051>.

Stevens, J.T., Haffey, C.M., Coop, J.D., Fornwalt, P.J., Yocom, L., Allen, C.D., Bradley, A., Burney, O.T., Carril, D., Chambers, M.E., et al., 2021. Tamm review: postfire landscape management in frequent-fire conifer forests of the southwestern United States. *For. Ecol. Manag.* 502, 119678. <https://doi.org/10.1016/j.foreco.2021.119678>.

Taylor, A.H., Trout, V., Skinner, C.N., Stephens, S., 2016. Socioecological transitions trigger fire regime shifts and modulate fire-climate interactions in the Sierra Nevada, USA, 1600–2015 CE. *Proc. Natl. Acad. Sci.* 113 (48), 13684–13689. <https://doi.org/10.1073/pnas.1609775113>.

Turner, M.G., Donato, D.C., Romme, W.H., 2013. Consequences of spatial heterogeneity for ecosystem services in changing forest landscapes: priorities for future research. *Landsc. Ecol.* 28 (6), 1081–1097. <https://doi.org/10.1007/s10980-012-9741-4>.

Vilanova, E., Mortenson, L.A., Cox, L.E., Bulaon, B.M., Lydersen, J.M., Fettig, C.J., Battles, J.J., Axelson, J.N., 2023. Characterizing ground and surface fuels across Sierra Nevada forests shortly after the 2012–2016 drought. *For. Ecol. Manag.* 537, 120945. <https://doi.org/10.1016/j.foreco.2023.120945>.

van Wagendonk, W.J., 2007. The history and evolution of wildland fire use. *Fire Ecol.* 3 (2), 3–17. <https://doi.org/10.4996/fireecology.0302003>.

Walker, B., Holling, C.S., Carpenter, S.R., Kinzig, A., 2004. Resilience, adaptability and transformability in social-ecological systems. *Ecol. Soc.* 9 (2). (<https://www.jstor.org/stable/26267673>).

Westerling, A.L., 2016. Increasing western US forest wildfire activity: sensitivity to changes in the timing of spring. *Philos. Trans. R. Soc. B Biol. Sci.* 371 (1696), 20150178. <https://doi.org/10.1098/rstb.2015.0178>.

Williams, A.P., Abatzoglou, J.T., Gershunov, A., Guzman-Morales, J., Bishop, D.A., Balch, J.K., Lettenmaier, D.P., 2019. Observed impacts of anthropogenic climate change on wildfire in California. *Earth's Future* 7 (8), 892–910. <https://doi.org/10.1029/2019EF001210>.

Williams, J.N., Safford, H.D., Enstice, N., Steel, Z.L., Paulson, A.K., 2023. High-severity burned area and proportion exceed historic conditions in Sierra Nevada, California, and adjacent ranges. *Ecosphere* 14 (1), e4397. <https://doi.org/10.1002/ecs2.4397>.

Willson, K.G., Margolis, E.Q., Hurteau, M.D., 2024. Trees have similar growth responses to first-entry fires and reburns following long-term fire exclusion. *For. Ecol. Manag.* 571, 122226. <https://doi.org/10.1016/j.foreco.2024.122226>.

Wood, S.N., 2017. *Generalized Additive Models: An Introduction with R*. Chapman and Hall/CRC.

Young, D.J.N., Meyer, M., Estes, B., Gross, S., Wuenschel, A., Restaino, C., Safford, H.D., 2020. Forest recovery following extreme drought in California, USA: natural patterns

and effects of pre-drought management. *Ecol. Appl.* 30 (1), e02002. <https://doi.org/10.1002/eaap.2002>.

Young, D.J.N., Stevens, J.T., Earles, J.M., Moore, J., Ellis, A., Jirka, A.L., Latimer, A.M., 2017. Long-term climate and competition explain forest mortality patterns under extreme drought. *Ecol. Lett.* 20 (1), 78–86. <https://doi.org/10.1111/ele.12711>.

Zald, H.S.J., May, C.J., Gray, A.N., North, M.P., Hurteau, M.D., 2024. Thinning and prescribed burning increase shade-tolerant conifer regeneration in a fire excluded mixed-conifer forest. *For. Ecol. Manag.* 551, 121531. <https://doi.org/10.1016/j.foreco.2023.121531>.

Ziegler, J.P., Hoffman, C.M., Collins, B.M., Knapp, E.E., Mell, W.R., 2021. Pyric tree spatial patterning interactions in historical and contemporary mixed conifer forests, California, USA. *Ecol. Evol.* 11 (2), 820–834. <https://doi.org/10.1002/ece3.7084>.